

Steady State Visual Evoked Potentials and the Visual Perception Curve

Jose Gustavo Berumen-Salazar
s1720783

Thesis
MSc in Psychology
Human Factor and Engineering Psychology

Coordinators

Ir. Tsvetomira K. Tsoneva
Philips Research Europe

Dr. Rob H. J. Van der Lubbe
University of Twente

Dr. Matthijs Noordzij
University of Twente

Dr. Gary Garcia-Molina
Philips Research North America

UNIVERSITY OF TWENTE.



Steady State Visual Evoked Potentials and the Visual Perception Curve

Master's thesis

to obtain the degree of
MSc in Psychology
Human Factors and Engineering Psychology

30 September 2016
Enschede, the Netherlands

Jose Gustavo Berumen-Salazar

s1720783

University of Twente
Philips Research Europe

Internal Coordinators

First Coordinator

Dr. Rob H. J. Van der Lubbe

University of Twente

Second Coordinator

Dr. Matthijs Noordzij

University of Twente

External Coordinators

Ir. Tsvetomira K. Tsoneva

Philips Research Europe

Dr. Gary Garcia Molina

Philips Research North America

**UNIVERSITY
OF TWENTE.**

Abstract

Repetitive visual stimulation (RVS), also known as flicker, induces oscillatory responses in the human visual cortex at the same, or harmonics of, the frequency of the stimulation. These responses are called Steady State Visual Evoked Potentials (SSVEP) are considered to be a strong and objective response of brain activity. SSVEP are used in research, clinical neuroscience and brain computer interfaces.

The amplitude of the SSVEP is influenced by the frequency and modulation depth (MD), contrast in light change, of the RVS. However, besides two studies conducted at Philips Research (Van de Sant, et al., 2011; Lazo, et al., 2013) we have no knowledge of research addressing the effect of frequency and MD on SSVEP. In particular the lowest MDs necessary to elicit SSVEP are unknown. Such knowledge could help developing better tasks eliciting SSVEP at different amplitudes which could increase the accuracy of SSVEP detection, their use for the evaluation of the visual system, and also increase their applications.

In order to study the effect of frequency and MD on SSVEP and to find the lowest MD necessary to elicit SSVEP we decided to use MDs around the Visual Perception Thresholds (VPT). The VPT are the lowest MD for a frequency at which people are able perceive flicker in RVS (Kelly, 1961; Perz, et al., 2011). We conducted an exploratory research where we evaluated a variety of frequencies (7-60 Hz) in combinations with MD at proportions (0.6 to 1.4) of the VPT in a RVS task. In addition, we combined the results of the two previously related Philips's studies in order to increase the possibilities to create a SSVEP contrast sensitivity curve, a curve with the values of the lowest MD necessary to elicit SSVEP.

We detected SSVEP for MDs around the VPT only for frequencies higher than 24 Hz and for MD lower the VPT. These SSVEP show an increase in amplitude with an increase in MD. We also created a SSVEP contrast sensitivity curve, which has a very similar shape to the VPC, especially for high frequencies. However, we did not find SSVEP at frequencies lower than 24 Hz, neither in our study nor in the two previous related studies. Our results indicate a close relationship between the VPC and the SSVEP contrast sensitivity curve, although the later may have higher MD for low frequencies.

Acknowledgements

I would like to express my most sincere appreciation to Tsvetomira for her continuous support during the entire project and for her great kindness. I am so grateful to have a supervisor who cared so much about my work, and who responded to my questions and troubles so promptly.

I would like to express my most sincere gratitude to Prof. Rob van der Lubbe for his always useful, accurate and constructive feedback, his thoughtful questions, and his kind and caring attitude towards me.

I would like to thank Prof. Matthijs Noordzij for his insightful comments and suggestions. I would also like to thank Prof. Gary Garcia-Molina, Björn Vlaskamp, Dragan Sekulovski and Gossia Perz, for their useful recommendations and feedback.

To the University of Twente for having granted me with the University of Twente Scholarship. This thesis and the completion of my master would have been impossible without it.

To Philips Research Europe for providing me all the facilities and resources to conduct this project and let me be part of their efforts.

To all my friends and colleagues at Philips: Andra, Kostas, Suvadeep, Tijmen, Kenta, Ada, Ioanna, Iris, and Yorick among others for making work fun.

To the participants who having more fun and less torturous things to do, they took selflessly part in the experiment with a big smile.

To my family, a mis padres y hermanas que siempre me han apoyado y dado más de lo que tienen sin esperar nada a cambio.

Table of contents

Abstract	iv
Acknowledgements	v
Table of contents	vi
List of figures	viii
List of tables	ix
Abbreviations	x
1 INTRODUCTION	1
1.1 Steady State Visual Evoked Potentials	1
1.2 SSVEP mechanisms.....	2
1.3 SSVEP neurophysiology.....	3
1.4 SSVEP characteristics.....	3
1.5 SSVEP applications	4
1.6 SSVEP limitations	5
1.7 SSVEP tradeoff strength and discomfort.....	5
1.8 Visual perception and SSVEP	6
1.9 The Visual Perception Curve and SSVEP	8
2 PURPOSE OF THE STUDY.....	9
2.1 Objectives of the study	9
2.2 Research questions.....	10
2.3 Hypothesis	10
3 METHODS	11
3.1 Participants	11
3.2 Inclusion and exclusion criteria	11
3.3 Ethical considerations	11
3.4 Materials	11
3.5 Stimuli.....	12
3.6 Stimulus selection and design.....	12
3.7 Experimental Task.....	14
3.8 Experimental session	15
4 DATA COLLECTION	16
4.1 Data pre-processing	16
4.1.1 Notch filter (50 Hz).....	17
4.1.2 Resampling	17
4.1.3 High pass filter (2 Hz)	17

4.1.4	Independent Component Analysis (ICA).....	18
4.1.5	Common Average Reference (CAR).....	19
4.1.6	Data segmentation and averaging	20
4.1.7	Identify events in photodiode signal.....	20
4.1.8	Epochs segmentation	21
4.1.9	Reject epochs.....	21
5	DATA ANALYSIS.....	23
5.1	Power Spectral Density (PSD).....	23
5.2	Z-scores.....	23
5.3	Equal Error Rate (EER)	24
5.4	Z-score at the Equal Error Rate (ZEER).....	24
5.5	Estimation methods for sensitivity curves	25
5.5.1	Absolute Modulation Depth (AMD) method.....	25
5.5.2	Psychometric method (PM)	26
6	RESULTS	27
6.1	SSVEP analysis	27
6.2	PSD.....	27
6.3	Z-scores.....	29
6.4	EER.....	31
6.5	ZEER	32
6.6	Sensitivity curves estimation for behavioral responses	34
6.6.1	AMD method for behavioral responses	34
6.6.2	Psychometric method for behavioral responses.....	35
6.7	Sensitivity curves estimation for SSVEP.....	37
6.7.1	AMD method for SSVEP	37
6.7.2	Psychometric method for SSVEP.....	38
6.7.3	SSVEP and Behavioral curves.....	39
6.8	SSVEP curves in the current and previous studies	40
6.8.1	SSVEP AMD curves for current and previous studies	40
6.8.2	SSVEP-Psychometric curves for current and previous studies	41
7	DISCUSSION.....	43
8	REFERENCES	46
9	APPENDIX A.....	50

List of figures

Figure 1.1 Fluctuation of luminance as a function of time for modulation depths of 100 and 50 percent.	6
Figure 1.2 Visual Perception Curves (VPC) for the flickering light.	7
Figure 1.3 The Visual Perception Curve and conditions in two previous related studies	8
Figure 3.1 Conditions employed in the current and two related experiments and the Visual Perception Curve	13
Figure 3.2 Structure of a trial in the flicker perception task. Repetitive Visual Stimulation (RVS)	14
Figure 3.3 A participant wearing the EEG cap and the experimental setup.	15
Figure 4.1 Steps in the pre-processing of EEG signal	17
Figure 4.2 Detection of the stimulation events in the photodiode signal.	21
Figure 4.3 Method to segment the epochs.	22
Figure 6.1 Power spectrum density average across all participants for each of the conditions at Pz site.....	28
Figure 6.2 Power Spectrum Density of Pz site averaged for all the participants at the frequency 60 Hz and Modulation Depth 1.4 times the Visual Perception Threshold.	30
Figure 6.3 Z-scores score average across subjects at channel Pz channels. Black vertical line represents the frequency of stimulation.....	28
Figure 6.4 Z-scores topo-plots average for all the participants for the 32 channels.....	31
Figure 6.5 Distribution of EER values for Pz site for all the participants by frequency.	32
Figure 6.6 Distribution of ZEER values for Pz site for all the participants by frequency.....	33
Figure 6.7 ZEER topo-plots average for all the participants for the 32 channels.....	34
Figure 6.8 Psychometric function and the underlying binomial distribution for all the frequencies and their corresponding modulation depths (MD).....	36
Figure 6.9. Visual Perception Curve and the Absolute Modulation and Psychometric Method curves for behavioral responses	37
Figure 6.10 ZEER-Psychometric function and the underlying binomial distribution for all the frequencies and their corresponding modulation depths (MD) for the Pz channel.	39
Figure 6.11 Visual Perception Curve, Absolute Modulation Depth Curve, Psychometric Curve, and SSVEP Psychometric Curve for Pz.	40
Figure 6.12 Visual Perception Curve, and Absolute Modulation Depth Method Curves of Van de Sant, et al., (2011); Lazo, et al., (2013); and Current study.....	41
Figure 6.13 Visual Perception Curve, and SSVEP Psychometric Curve of Van de Sant, et al., (2011); Lazo, et al., (2013); and Current study.	42

Figure 9.1 Power spectrum density average across all the subject for each of the conditions at Oz site.....	51
Figure 9.2 Z-scores score average across subjects at channel Oz channels.....	52
Figure 9.3 Distribution of EER values for Oz site for all the participants by frequency. Boxplots.....	53
Figure 9.4 Distribution of ZEER values for Oz site for all the participants by frequency	54
Figure 9.5 ZEER-Psychometric function and the underlying binomial distribution for all the frequencies and their corresponding modulation depths (MD) for the Oz channel.....	56
Figure 9.6 SSVEP-Psychometric Curve for Oz and the Visual Perception Curve	57

List of tables

Table 3.1 Absolute values of modulation depth for each frequency in the experimental task	13
Table 6.1 Average number of “yes” for all participants per condition	35
Table 6.2 Average number of trials with ZEER values greater than 0 for Pz site.....	38
Table 9.1 Average number of trials with ZEER values greater than 0 for Oz site	55

Abbreviations

AMD	Absolute Modulation Depth
BCI	Brain Computer Interfaces
CAR	Common Average Reference
DC	Direct Current
EEG	Electroencephalography
EER	Equal Error Rate
FFT	Fast Fourier Transforms
ICA	Independent Component Analysis
MD	Modulation Depth
PSD	Power spectrum density
RVS	Repetitive Visual Stimulation
SSVEP	Steady State Visual Evoked Potentials
VPC	Visual Perception Curve
VPT	Visual Perception Threshold
ZEER	Z scores for Equal Error Rates

1 Introduction

The Steady State Visual Evoked Potentials (SSVEP) are electrical responses of the brain to rapid repetitive stimulation (RVS), also known as flicker. SSVEP are used in research and practical applications because it is a stable response and reflects characteristics of the stimulation. The SSVEP is detected at the same frequency, or harmonics, of the driving stimulation. One way to elicit SSVEP is by flickering light tasks where variations in the frequency and modulation depth (MD), a measure of light change, of the stimuli are associated with changes in the SSVEP. However, despite the long history of research on visual perception and on SSVEP, the effects of frequency and MD on SSVEP are not well addressed and in particular it still unknown the lowest MD at which SSVEP can be elicited. Such knowledge will allow to create better tasks to elicit SSVEP and with that potentially increase the accuracy of SSVEP detection, their use to study the visual system and increase their applications.

This work aimed to find the lowest MD necessary to elicit SSVEP for a variety of frequencies between 7 and 60 Hz. For this pursue, we used MD proportions (0.6 to 1.4) of the Visual Perception Thresholds (VPT), the lowest MD at which people can perceive flicker in the light stimulation. During the task participants had to indicate whether or not they perceived flicker in light stimulation while simultaneously an electroencephalogram (EEG) was recorded. We analyzed the EEG data to characterize and measure the strength of the SSVEP. In addition, we incorporated the results of two earlier related studies in order to increase the number of frequencies and contribute to create a curve with the lowest MD necessary to elicit SSVEP.

1.1 Steady State Visual Evoked Potentials

Steady State Visual Evoked Potentials (SSVEP) are electrical brain responses associated with the stimulation of the retina by rapid repetitive visual stimulation (RVS), e.g., flickering light (Regan, 1977). The main distinctive characteristic of SSVEP is that they contain high power at the same at the frequency of stimulation and/or harmonics thereof (Regan, 1989). SSVEP have a very stable amplitude (size) and phase (temporal shift) over time (Regan, 1966) and are most prominent over occipital cortical areas (Vialatte, Maurice, Dauwels, & Cichocki, 2010). SSVEP are usually obtained by means of electroencephalographic (EEG) recordings, however they are also obtained by means of magnetoencephalogram (Thorpe, Nunez, & Srinivasan, 2007) and functional magnetic resonance imaging (Sammer, et al., 2005). SSVEP can be

elicited in the absence of a behavioral response and even when participants are not able to consciously perceive the flicker (Skrandies, & Raile, 1989).

1.2 SSVEP mechanisms

The nature of the mechanisms that generate SSVEP is still unknown. However, there are two hypothesis that attempt to explain the possible mechanisms underlying SSVEP. These hypothesis have two different perspectives of SSVEP; they considered SSVEP to be either the result of spontaneous or evoked oscillations in the brain.

One hypothesis suggests that SSVEP are the result of the enhancement of the spontaneous oscillations of the brain. This proposes that with RVS stimulation the brain stops producing its spontaneous neural activity and enters into an entrained state where neurons synchronize their firing to the stimuli frequency preventing the brain to return to its spontaneous activity while the stimulation its present (Regan, 1989). This could be explained by the resonance phenomena, the behavior of neural oscillators of the brain to match stronger some of their ongoing responses to certain frequencies of period stimulation (Silberstein, 1995, as cited in Bayram, et al., 2011). In one study, dedicated to evaluate this hypothesis, frequencies from 1 to 100 Hz with an increase of 1 Hz were tested in a flicker perception task (Herrmann, 2001). It was found that participants present stronger responses to 10, 20, 40 and 80 Hz compared to the other frequencies, even when the stimuli at these frequencies were not different to the rest of the stimuli. This results suggest that SSVEP could be the result of tuning of ongoing oscillations of the brain to certain frequencies.

The second hypothesis suggests that SSVEP are the result of induced responses provoked by stimulation. According to this this hypothesis SSVEP might be the result of the addition of individual and small transient responses, such as Event-Related Potentials (ERPs), generated by each stimulus (Capilla, Pazo-Alvarez, Darrriba, Campo & Grosss, 2011). This is similar to explanation of the generation of early ERPs by phase resetting behavior of neurons (shifts in their dynamic oscillations) instead of additive amplitude changes (Makeig et al., 2002). A recent study found that SSVEP could be explained by phase resetting (Moratti, Clementz, Gao, Ortiz, & Keil, 2007). In that study the changes on amplitude and phase, associated with SSVEP, before and after the start of stimulation were tracked. They found few changes in amplitude but a strong phase alignment, which suggest that phase alignment could be the main mechanism for SSVEP generation.

1.3 SSVEP neurophysiology

The three components of the visual system - the retina, the visual path and the visual cortex - are expected to be involved in the generation of the SSVEP. However, due to the low spatial resolution of the EEG, which is the main technique for obtaining SSVEP, the mechanisms in the visual cortex and in the rest of the visual system are vastly unknown. According to Vialatte and colleagues (2010) the three main visual pathways - the magnocellular, the parvocellular and the koniocellular – take part in the generation of the SSVEP. The three pathways start in the retina continue to the lateral geniculate nuclei and project to the visual areas, in particular the striate cortex (V1), which is considered to be the strongest local source for SSVEP (Vialatte, et al, 2010). LGN activation has been found to be associated with the generation of SSVEP (Krolak-Salmon et al., 2003).

SSVEP could also have contribution from other cortical and subcortical regions, from the primary visual cortex the SSVEP could propagate to other brain areas. This idea is supported by the findings that regions beyond the visual system are activated during SSVEP, these areas include parietal and frontal brain areas (Srinivasan, Bibi, & Nunez, 2006; Pastor, Valencia, Artieda, Alegre, & Masdeu, 2007) and the cerebellum (Pastor, Artieda, Arbizu, Valencia, & Masdeu, 2003). It appears that SSVEP manifest in an occipito-frontal network that is connected to certain extra-cortical structures (Srinivasan, Fornari, Knyazeva, Meuli, & Maeder, 2007).

1.4 SSVEP characteristics

SSVEP have several distinctive properties that make them a strong and objective measure of brain response: a) the experimenter has control over the SSVEP as one can manipulate variables that affect the SSVEP such as spatial frequency, luminance, and hue (Di Russo, Spinelli, & Morrone, 2001), b) SSVEP are less susceptible than ERPs to artifacts produced by eye movements (Perlstein, et al., 2003) and to electromyographic noise contamination (Gray, Kemp, Silberstein, & Nathan, 2003) c) SSVEP are an implicit response as they do not require a motor response to be elicited and as a result are not highly influenced by effects after sensory or perceptual encoding stages (Skrandies, & Raile, 1989), d) they have a high signal to noise ratio (SNR) particularly in occipital sites as only a fraction of the noise contained in the EEG affects the SSVEP frequency related to the stimulus and at high frequencies the noise is lower than at low frequencies (Norcia, et al., 2015), and e) SSVEP are considered to be an ecological

valid measure of brain activity as they are elicited by a continuous sustained visual experience rather than by an isolated stimulus (Di Russo, et al., 2007).

1.5 SSVEP applications

The above distinctive characteristics make SSVEP very useful for research and also practical purposes. In cognitive neuroscience, SSVEP are often used to indirectly estimate the propagation of brain activity on a cognitive task (Vialatte, et al., 2010). Some cognitive processes that have been studied through the use of SSVEP include visual attention (Morgan, Hansen, & Hillyard, 1996), binocular rivalry (Müller, et al., 1998) and working memory (Perlstein et al., 2003). In clinical neuroscience SSVEP are used as a diagnostic tool to study pathological brain dynamics. For instance, it was found that the magnocellular pathway is affected in patients with Alzheimer. This was found by evaluating the visual system with the use of SSVEP elicited by stimulation at high frequencies (Sartucci, et al., 2010).

However, by far the main practical application of SSVEP is in the field of Brain Computer Interfaces (BCI). The objective of BCI is to establish a direct communication between a brain and a computer that allows a person to control or communicate with a device without muscular intervention (Van Erp, Lotte, Tangermann, 2012). The main reason SSVEP are used in BCI is because the frequency of the stimulation can be reliably and quickly recognized in the SSVEP frequency domain. Other characteristics that make SSVEP very suitable for BCI are that they have a very high temporal resolution for data acquisition (~0.05 seconds; Nicolas-Alonso, & Gomez-Gil, 2012), people require minimal training to perform a SSVEP task (Vialeto, et al., 2010), the cost of the SSVEP necessary equipment is low compared with other neuroscience techniques (Luck, 2014), there are years of research on SSVEP and BCI (Norcia, et al., 2015), and SSVEP allow people a relatively free movement of their head and eyes compared with other neuroscience methods such as eye tracking.

A common example of a SSVEP-based BCI application is the control of a wheelchair. In a BCI-controlled wheelchair system, four sources of light can be associated with four directions: up, down, right and left. When a person wants to move the chair in a certain direction they need to attend the light stimulus associated with that command. The computer program would analyze the brain activity, identify the frequency of the SSVEP and send the command to the wheelchair with the direction that the person intended (Bi, Fan, & Liu, 2013).

1.6 SSVEP limitations

Despite the strengths of the SSVEP, they also have some side effects and disadvantages. One disadvantage of SSVEP is the possibly harmful side effects of the exposure to fluctuating light. It has been documented that a few seconds of exposure to flickering light with bright colors at low to medium frequencies can trigger epileptic seizures (Fisher, Harding, Erba, Barkley, & Wilkins, 2005). One of the most infamous cases is the one of the Japanese cartoon "Pokémon". In an episode repetitive visual stimuli induced photosensitive epileptic seizures in hundreds of viewers (Ishiguro, et al., 2004). Furthermore, high frequencies may also have other undesirable effects. It has been reported that long (5 minutes or more) and continuous exposure to flickering light at unperceivable high frequencies can induce migraines (Vanagaite, et al., 1997) or impaired visual performance in an office environment (Kuller, & Laike, 1998).

The influence of sensorial and cognitive processing on the perception of RVS and subsequently on SSVEP are also not very well addressed. Habituation and attention are only two examples of processes that can influence SSVEP. Prolonged view of flickering stimulation at a particular frequency causes adaptation (Pantle, 1971), which can already reduce the EEG amplitude (Bergholz, Lehmann, Fritz & Rüter, 2008). The perception sensitivity to RVS at low or medium frequency (e.g., 30 Hz) can be reduced to by adaptation to a higher unperceivable flickering stimulation (e.g., 60 Hz) (Shady, MacLeod, & Fisher, 2004). Visual attention is also associated with pupil dilation which could increase retinal luminance and affect the effectiveness of an SSVEP stimulus (Janisse 1997 in Silberstein, et al., 1990). SSVEP are also enhanced by selective attention to an attended versus and unattended stimulus (Morgan, Hansen, & Hillyard, 1996).

1.7 SSVEP tradeoff strength and discomfort

For SSVEP based BCI applications and to reduce the possible side effects of flickering light, the RVS is preferred to elicit strong SSVEP responses, while not causing visual discomfort to people. It should be pointed out that this is not always the case, for instance in for clinical applications where the goal is to test integrity of the visual pathway like in patients who suffered epileptic seizures, RVS may be preferred to cause discomfort to people (Trenité, Binnie, & Meinardi, 1987). The case of RVS for SSVEP-based BCI is a difficult endeavor, due to the fact that both stimulation at low and high frequencies have their advantages and disadvantages. Stimulation at low frequencies at high MD (higher than the MD in the VPT) can cause

discomfort as people can perceive the flicker, however the SSVEP amplitude is greater for low frequencies stimulation, particularly around the EEG alpha range (8–13 Hz), where the SSVEP signal has the highest amplitude (Regan, 1989). On the other hand stimulation at high frequencies and at medium to low MD (smaller than the MD at the VPT) are less uncomfortable to people as the stimulation is perceived as continuous, but this frequency range and MD induces weaker or no SSVEP responses (Van de Sant, et al., 2011).

1.8 Visual perception and SSVEP

SSVEP are very sensitive to characteristics of the stimulus such as spatial frequency, luminance, and color (Di Russo, Spinelli, & Morrone. 2001). Among those characteristics, the frequency and MD are particularly relevant as they modulate the amplitude of SSVEP (Regan, 1989). The frequency measured in (Hz) is the number of repetitions of the stimulus per unit of time (seconds). MD is a measure of light variation that quantifies the relation between the spread and sum of two luminances during period oscillations (Perz, et al., 2011). For a time-varying luminance, such as flickering light, MD is an indication of the ratio between the average light level and the amount of change in the light and can be calculated according to the equation 1.1. In addition, the concept can be visualized in Figure 1.1.

$$MD = \frac{L_{max} - L_{min}}{L_{max} + L_{min}} * 100 \quad \text{Eq. 1.1}$$

where:

MD = Modulation Depth

L_{max} = maximum luminance

L_{min} = minimum luminance

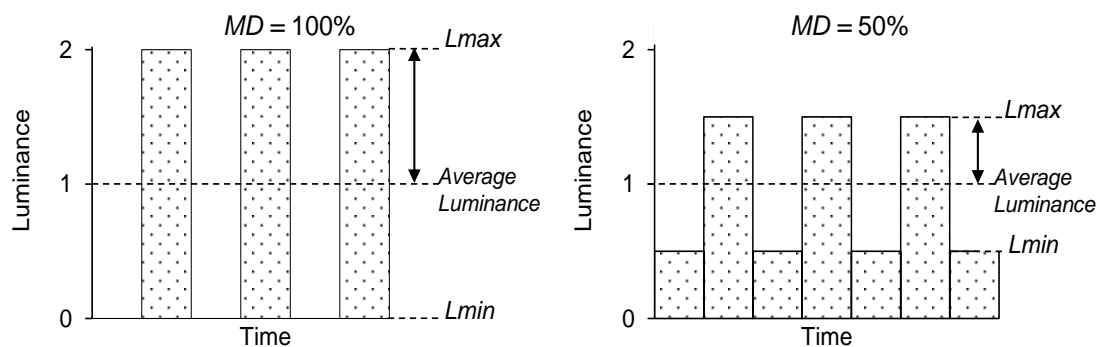


Figure 1.1. Fluctuation of luminance as a function of time for modulation depths at 100 and 50 percent. Adapted from "Electrical and psychophysical responses of the human visual system to periodic variation of luminance," by S., Sokol, and L.A. Riggs, 1971, *Investigative Ophthalmology & Visual Science*, 10(3), p. 173.

In addition, frequency and MD determine the human perception of RVS and such relationship is described by the temporal contrast sensitivity function (Kelly, 1961). The curve is known as Visual Perception Curve (VPC) and it defines the Visual Perception Threshold (VPT) in terms of frequency and MD. A VPT is the lowest MD for a particular frequency at which people can perceive RVS as discontinuous. Usually people perceive as discontinuous stimulation RVS with MD on and above the VPT and as continuous stimulation RVS with MD below the VPT. From frequencies above 10 Hz the VPC has an increase in MD with an increase in frequency. For instance, at low frequencies (e.g., 10 Hz) only small changes in MD are necessary for people to detect the RVS as discontinuous. While at high frequencies (e.g., above 40 Hz), higher MD are required for people to detect the RVS as discontinuous (Figure 1.2).

A more recent version of the VPC, using the entire visual field and controlling for adaptation was created recently at Philips Research (Perz, Sekulovski, & Vogels, 2011). The recent VPC has a similar shape to the Kelly’s curve (1961), but it has lower VPTs. The two curves can be seen in Figure 1.2.

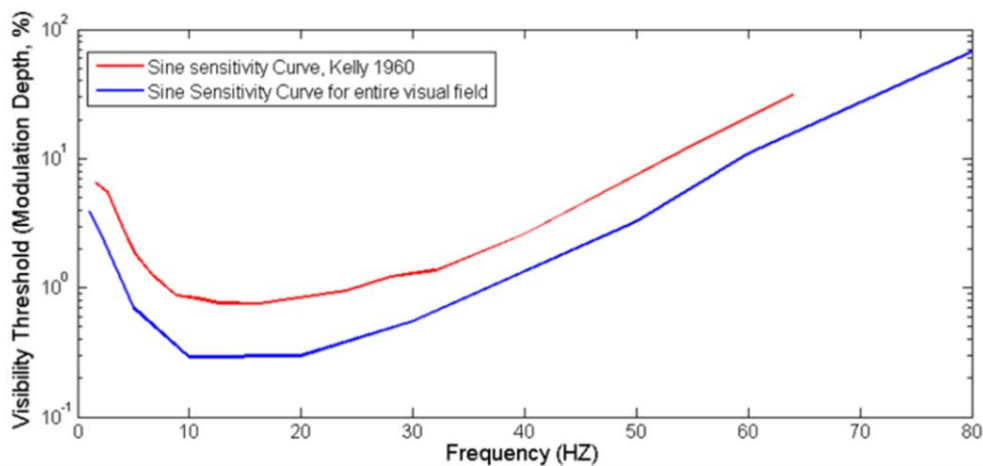


Figure 1.2. Visual Perception Curves (VPC) for the perception of flickering light. The red line correspond to the VPC of Kelly (1961) and the Blue line to the VPC of Perz, et al., (2011). Reprinted from “Flicker perception,” by M. Perz, D. Sekulovski, and I. Vogels, 2011, *Philips Research Europe Technical Note*, p. 20.

We consider the VPC by Perz and colleagues (2011) to be more appropriate than the VPC by Kelly (1961) for our study because of the following reasons: Perz and colleagues evaluated the a visual field of 137° in a binocular experiment instead of the only 65 ° in Kelly’s monocular experiment, they controlled for adaptation in the experimental task as they used a staircase detection task, instead of the tuning methodology of Kelly. In the Perz and colleagues

detection task MD increased or decreased until the participant response change from “yes” to “no” or vice-versa which prevent for adaptation. In both studies stimuli were presented centrally on the retina. Moreover, the Perz’s study has an additional advantage for our study, we can use the same setup they used because their equipment is at our disposal at Philips Research, and that set up has been used in related relevant studies.

1.9 The Visual Perception Curve and SSVEP

To our knowledge there are few studies that investigated how the frequency and MD of the RVS affect the SSVEP (Van de Sant, et al., 2011; Lazo, et al., 2013). Van de Sant et al. (2011) exposed participants to RVS light at frequencies of 8, 24, 32, 40 and 48 Hz and MD of 0.6, 0.8, 1.0, 1.2, 1.4 times the VPT in Kelly’s VPC (1961). They found SSVEP for all the frequencies, except 8 Hz, at MD starting below the VPT. In the second study, Lazo et al. (2013) investigated five frequencies 6, 24, 32, 40, 60 Hz at five absolute MDs 0.002, 0.008, 0.014, 0.020, and 0.026. They found SSVEP only for the frequencies 24 and 32 Hz at MD starting at 0.008 and for 40 Hz at MD starting at 0.002. SSVEP were not found for the lowest frequency 7 Hz, nor for the highest frequency 60Hz. A visual representation of the conditions in these two studies can be seen in Figure 1.3.

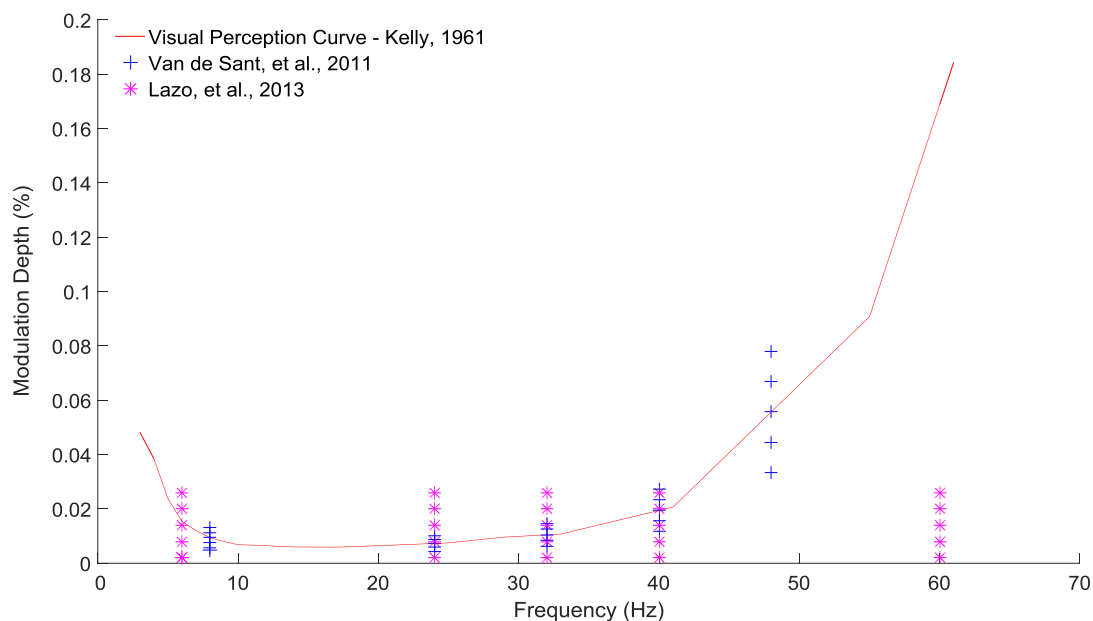


Figure 1.3. The Visual Perception Curve (Kelly, 1961) and conditions in two previous related SSVEP studies. Blue crosses represent the conditions tested in Van de Sant et al. (2011) while pink stars correspond to the conditions in Lazo et al. (2013).

2 Purpose of the study

Since the first time SSVEP were characterized (Adrian & Matthews, 1934), they have been a useful tool to study the brain activity associated to visual perception (Reagan, 1989) and in the last decade their use have increased to more practical applications (see a review Norcia, et al, 2015). However, one issue concerning SSVEP that has not been addressed is regarding the neural model describing the human sensitivity to the perception of RVS. The effect of frequency and MDs and in particular the value of the lowest MD necessary to elicit SSVEP are unknown. That knowledge could help increasing the accuracy of SSVEP detection and help to develop better models to evaluate the visual system and also increase their applications. However, besides the two studies conducted at Philips Research we have no knowledge of research addressing this issue.

We considered that investigating the effect of the driving frequency on SSVEP and in particular finding the lowest MD necessary to elicit SSVEP are particularly relevant for the research and the practical application of SSVEP. That can help to develop better task minimizing any adverse effect from RVS.

2.1 Objectives of the study

We aimed to study the effect of frequency and MD on SSVEP and to find the lowest MDs necessary to elicit SSVEP for frequencies in the range of the VPC (1 to ~70 Hz) and with that help to create a SSVEP contrast sensitivity curve, a curve with the values of the lowest MD necessary to elicit SSVEP for a wide range of frequencies. We also aim at examining the interaction between different range of frequencies (low, medium and high) and MD (below, at and above the VPT) and find if they affect SSVEP in a similar manner as in the visual perception research: an increase in frequency requires an increase in MD.

Thus, we have three goals in this study. The first goal is to investigate it is possible to elicit SSVEP around the VPC, and if so for what frequencies and MDs. In particular we are interested to find the lowest MD necessary to elicit SSVEP. The second goal is to examine how the interaction between frequency and MD affect SSVEP. The third goal is to create a SSVEP contrast sensitivity curve by combining our results with the two previous related studies.

We intend to use the Perz's VPC (Perz, et al, 2011) as we mentioned in the introduction section is better suited for our study than the Kelly's VPC (Kelly, 1961). From here on, we will refer to the Perz's VPC only as VPC.

2.2 Research questions

1. Is it possible to elicit SSVEP with MDs proportions (0.6 to 1.4) of the VPT for frequencies in the range of 7 to 60 Hz by RVS light? If yes, for what frequencies and MDs and what are the lowest MDs necessary to elicit SSVEP?
2. How do the frequency and MD of the RVS affect SSVEP?
3. Is the SSVEP contrast sensitivity curve similar to the VPC?

2.3 Hypothesis

1. SSVEP are elicited by RVS with MDs around the VPT. However this occur only for MDs that are equal of higher than the VPT for SSVEP. The lowest MDs necessary to elicit SSVEP are above the VPT of the VPC.
2. There is an interaction between frequency of stimulation and MD: an increase in frequency requires an increase in MD to elicit SSVEP. We expected the SSVEP-VPC follows a similar pattern to the VPC.
 1. The MD necessary to elicit SSVEP at high frequencies is higher than the VPT at low frequencies.
 2. There is a high increase in MD necessary to elicit SSVEP for frequencies higher than 30 Hz as in the VPC.
3. The SSVEP contrast sensitivity curve has a similar shape to the VPC. However, the VPT in the SSVEP contrast sensitivity curve are higher than the VPT in the VPC.

3 Methods

We created RVS light perception task with 6 different frequencies in three frequency ranges low, medium and high (7, 13, 19, 37, 48 and 60 Hz) combined with 5 MD proportions of the VPT (0.6, 0.8, 1.0, 1.2, and 1.4).

3.1 Participants

The group of participants consisted of 24 healthy volunteers (17 males and 7 females, Mean age = 26.4; SD = 6.0). The participants were recruited among the Philips Research employee population at High Tech Campus, Eindhoven. All participants had normal or corrected to normal vision. At the end of the experiment participants were rewarded with chocolate and a hair wash coupon to remove the gel used during EEG recording. Three additional participants were excluded from the final group due to problems with the EEG recording (n =2) or recording the RVS events (n = 1).

3.2 Inclusion and exclusion criteria

In order to be included in the study, participants had to be between 20 to 50 years old. They also had to be healthy: no vision related problem, no history of epilepsy, neurophysiological disorder, migraine, or sleep problems. Participants were excluded in case of: colorblindness, suspicion or report of an aberrant light sensitivity, photosensitizing medication, sleep disorders or visual impairments.

3.3 Ethical considerations

The research protocol was approved by the Philips Research Ethics committee board (Internal Committee Biomedical Experiments). Prior to the study, participants received a consent letter with all details related to their involvement in the study. At the start of the study the participants signed the letter.

3.4 Materials

The experimental setup consisted of the following hardware: a) 2 LED panels 57.5 cm x 57.5 cm equipped strips of white lamps, b) Agilent N3300A System DC Electronic Load, c) Agilent 33522A Function Generator, d) BioSemi Active Two EEG signal acquisition system, e) 32

electrode setup placed on a textile cap according to the international 10-20 system, f) Photodiode, g) Laptop with Windows 7 operating system, h) 18-Key USB Numeric Keypad.

The RVS light was presented via a custom made program in JAVA. The waveform specifications were sent to the Agilent 33522A function generator and then to the LED panels using the TCP/IP interface. Once the waveforms were created, they passed through the Agilent N3300A System DC Electronic Load in order to regulate the current load before they reached the lamps. The light stimulation was reflected on a white wall with a fixation cross in the middle. The participants were instructed to look at the fixation cross during the experiment. The USB numeric Keypad was connected to the Laptop to receive the input from the participants. The BioSemi ActiveTwo EEG Acquisition System recorded the EEG and the light stimulation signals via the use of an EEG cap and a photodiode respectively. All data were saved on the laptop.

3.5 Stimuli

The light stimulation was delivered via two LEDs panels with a size of 57.5 cm x 57.5 cm and equipped with four rows of cold warm white LEDs. For this experiment only the cold LEDs were used. The LEDs panels were suspended on a stand at a height of 2.5 and illuminated a white wall in front of the participant. The LEDs panels were controlled via an Agilent function generator. The system was calibrated to ensure that the correct output was delivered. The light stimulation covered a total area of approximately 210 cm x 360 cm (vertically x horizontally). Participants were at a distance of 70 cm and have a visual angle of 137°. These devices for light stimulation resemble the conditions of a typical office and have worked properly in previous experiments at Philips Research.

3.6 Stimulus selection and design

The 30 conditions were created from the combination of 6 frequencies (7, 13, 19, 37, 48 and 60 Hz) and 5 MD (0.6, 0.8, 1.0, 1.2, and 1.4) times the corresponding VPT of each frequency at the VPC. The absolute values of the MD are listed in Table 3.1.

The selection of these frequencies and MDs was motivated by our aim to combine our results with the two previous related studies (Van de Sant, et al., 2011; Lazo, et al., 2013), which allowed us to have more conditions around the VPC. The conditions of the previous and our experiment can be seen in Figure 3.1. We selected our conditions to cover low (<12 Hz),

medium (12-30 Hz) and high frequencies (>30 Hz), and to cover areas that were not covered in the previous studies.

Table 3.1

Absolute values of modulation depth for each frequency in the experimental task

MD	Frequency (Hz)					
	7	13	19	37	48	60
0.6x VPT	0.00272	0.00106	0.00098	0.00650	0.01443	0.03826
0.8x VPT	0.00363	0.00142	0.00130	0.00867	0.01924	0.05102
1.0x VPT	0.00453	0.00177	0.00163	0.01084	0.02405	0.06377
1.2x VPT	0.00544	0.00212	0.00195	0.01301	0.02886	0.07652
1.4x VPT	0.00635	0.00248	0.00228	0.01517	0.03367	0.08928

Note. MD = Modulation Depth; VPT = lowest MD at which participants perceive RVS as discontinuous, the values were obtained from the Visual Perception Curve (Perz, et al., 2011); x = times, for instance 0.6x VPT is equal to 0.6 times the VPT

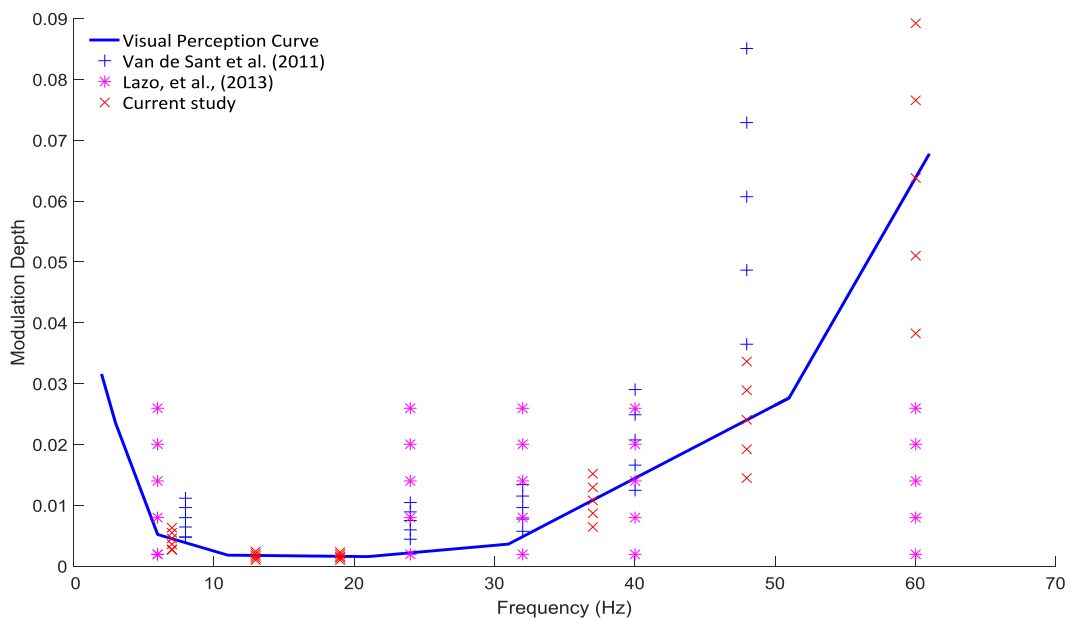


Figure 3.1. Conditions employed in the current and two related experiments and the Visual Perception Curve. Blue line correspond the Perz's Visual Perception Curve (Perz, et al, 2011). Blue crosses represent the conditions in Van de Sant et al., 2011, pink stars represent the conditions used in Lazo et al., 2013, red cross marks represents the conditions in the current study.

We chose in this study square waves, instead of sine waves, because square waves were used in the two previous related studies we intended to combine our results and because square

waves have a higher accuracy than sine waves for eliciting SSVEP at the frequency of stimulation (Teng, et al., 2011). The waves had a duration of 3 seconds (6248 samples at a sample rate of 2048Hz). The average light luminance level was 1000 Lux and the color temperature was 4000 K. The waveforms were created using the following equation:

$$\text{Waveform} = AvLL + \text{square}(T * F) * MD * AvLL \quad \text{Eq. 3.1}$$

where:

AvLL = Average Light Level

square () = square waves

T = Time (seconds)

F = Frequency (Hz)

MD = Modulation Depth (%)

3.7 Experimental Task

The experimental task consisted of 300 trials that were the result of 30 RVS waveforms that were repeated 10 times each. A trial consisted of 3 seconds of continuous light, followed by a beep and 3 seconds of RVS which were followed by 2 beeps and a period of continuous light that continued until the participant gave a response. See Figure 3.2 for a visual representation of one trial.

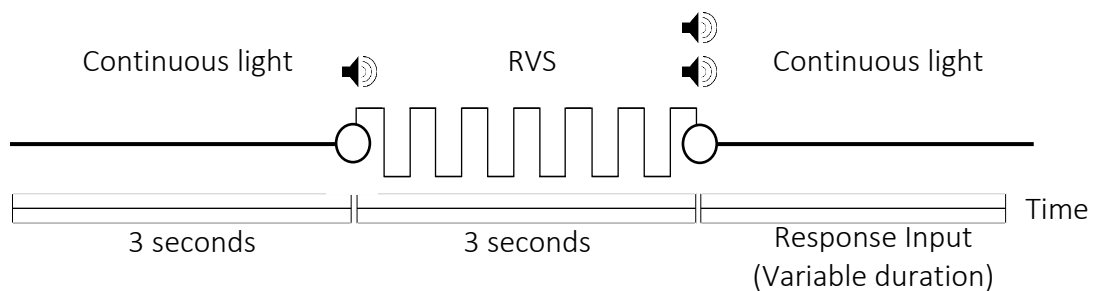


Figure 3.2. Structure of a trial in the flicker perception task. Repetitive Visual Stimulation (RVS).

The trials were randomly organized for each participant in three blocks of 100 stimuli. Each block lasted approximately 14 minutes and was followed by a break of a variable duration (3-10 minutes). Participants respond whether or not they perceived flicker by pressing “yes” or “no” stickers over the buttons on a number pad (6 for “yes” and 4 for “no”).

3.8 Experimental session

The study consisted of one experimental session of approximately one hour and fifteen minutes. At the beginning of the session the experimental leader explained the goal of the study and answered any questions that participants had regarding the procedures to be conducted during the session. After that participants were seated comfortably on a chair in front of the white wall where the light was reflected. Then, we proceeded with placing an EEG cap on the head of the participant, and added conductive gel to the electrodes. Next, we measured the impedances of the EEG signal, and made sure the impedances of all the channels were below $20 \mu V$.

Once the EEG cap was set, participants were again explained the task they needed to perform and were allowed to do a short practice run. During the experiment participants were instructed to look with their two eyes open at a fixation cross on the middle of the wall. Between blocks participants had a break where they had the opportunity to relax and drink some water. At the end of the session the experimental leader answered any questions that the participants had regarding the experiment. Also, the experimental leader gave the participants a chocolate and a hair wash coupon to remove the gel left in their hair.



Figure 3.3. A participant wearing an EEG cap and the experimental setup. The picture depicts the two LED panels are above and the white wall in front of the participant.

4 Data collection

Electrical brain activity was recorded from 32 scalp sites (Fp1, AF3, F7, F3, FC1, FC5, T7, C3, CP1, CP5, P7, P3, Pz, PO3, O1, Oz, O2, PO4, P4, P8, CP6, CP2, C4, T8, FC6, FC2, F4, F8, AF4, Fp2, Fz, and Cz) positioned according to the international 10-20 system using an elastic cap. The signals were recorded at a sampling rate of 2048 Hz using the BioSemi™ ActiveTwo signal acquisition system (BioSemi products, 2016, July 16). Two additional electrodes, a Common Mode Sense active electrode and Driven Right Leg passive electrode were used to replace the ground and references electrodes respectively.

The flickering light was recorded using a photodiode that recorded the variations of the light reflected in the wall. Large variations in the average light were used to identify the start and the end of the trials. After the experiment, the events were detected in the photodiode. Then, the time of the start and the end of the events were marked in the EEG signal. This process is explained later in the preprocessing section. The photodiode was placed in a small table at the left side of the participants at a distance of approximately 70 cm to the wall. In addition, the behavioral responses of the participants were logged in a text file together with the frequency and MD of the corresponding trial.

4.1 Data pre-processing

EEG and light signals were preprocessed using EEGLAB (Delorme & Makeig, 2004) and custom-made MATLAB scripts. We followed the procedures employed in the two previous related studies (Van de Sant, et al., 2011; Lazo, et al., 2013). Signals were notch filtered at power-line frequency (50Hz) and then re-sampled at 256 Hz. Then, signals were high pass filtered at 2Hz and blinks components were removed by Independent Component Analysis (ICA). After that signals were referenced to common average reference (CAR) excluding T7 and T8 channels. Finally, the data was separated into non overlapping epochs. The preprocessing steps are presented in the Figure 4.1.

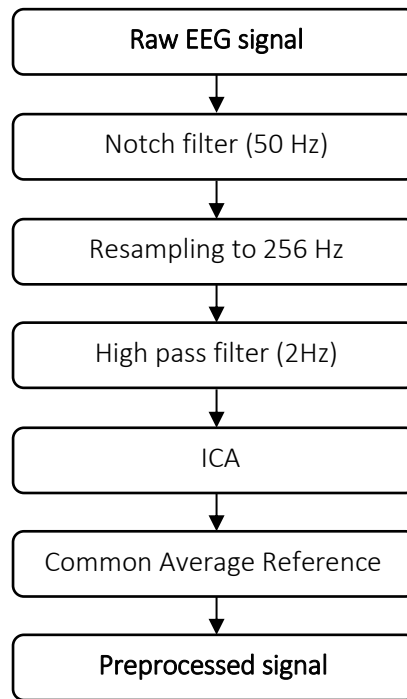


Figure 4.1. Steps in the pre-processing of EEG signal

4.1.1 Notch filter (50 Hz)

The preprocessing started by removing the external noise that comes from the AC power line. For this purpose we applied a notch filter at 50 Hz to remove the external noise coming from the AC power line.

4.1.2 Resampling

The original rate of the recording of each measurement point, called sample, was at 2048 Hz. This implies that for each second we had 2048 points of information, which requires a long time for processing. So as to reduce the time necessary to process the signal, we resample from the original 2048 Hz to 256 Hz.

4.1.3 High pass filter (2 Hz)

The EEG signal below 2 Hz is often affected by drifts in the impedance of electrodes and sweating. In order to reduce those effects a high pass filter with a cutoff at 2 Hz was applied by a linear-phase finite impulse response (FIR) filter to eliminate DC shifts (Widmann, Schröger, & Maess, 2015).

4.1.4 Independent Component Analysis (ICA)

The EEG signal is susceptible to eye blinks and other artifacts, which represents an issue to its adequate interpretation and analysis. The ICA technique separates the different sources of the EEG signal and with that helps to remove the contribution of these artifacts. For ICA we followed the procedure employed by Lazo, et al., (2013), the equations presented below were taken and adapted from their study. The artifact correction extracts from the recorded signal the information that corresponds exclusively to cerebral sources. The signal can be represented as the following equation:

$$EEG_{rec}(t) = EEG_c(t) + \sum_{n=1}^N EEG_n(t) \quad \text{Eq. 4.1}$$

where:

- $EEG_{rec}(t)$ = recorded EEG signal
- $EEG_c(t)$ = signal from cerebral sources
- $EEG_n(t)$ = signal from artifactual sources

ICA is a blind source separation method that enables representing the data as a linear combination of statistically independent signals (sources). The artifact components of an EEG signal can be estimated by ICA, if we assume that the potentials of artifacts in EEG are independent from cerebral EEG potentials, the artifacts and signals. ICA can be explained with the cocktail-party problem (Hyvärinen, Karhunen, & Oja, 2001) and the signal can be modeled according to the following equation:

$$x_i(t) = a_{i1}s_1(t) + a_{i2}s_2(t) + \dots + a_{in}s_n(t) \quad \text{Eq. 4.2}$$

for all $i = 1, \dots, n$,

where:

- n : number of people speaking simultaneously in a room and number of microphones
- $x_i(t)$: microphone measure
- $s_n(t)$: speech signal emitted by the speaker
- a_{ij} : distance (parameter) between the microphones and speakers

The goal is to estimate the mixing components and coefficient from the recorded signal. The model can be written as follows:

Eq. 4.3

$$x = Ms$$

The components $s_i(t)$ are inversely given by:

$$x = \sum_{i=1}^n a_i s_i \quad \text{Eq. 4.4}$$

where:

x = is a vector with $x_1(t), \dots, x_n(t)$ as elements

M = is an $n \times n$ Matrix with $a_1(t), \dots, a_n(t)$ as elements

s = is a vector with $s_1(t), \dots, s_n(t)$ as elements

Then, by assuming certain restrictions on s and M it is possible to estimate them. The assumptions of ICA on the sources s_n are:

1. All the sources are mutually independent to estimate W
2. All but one component must have non-Gaussian distributions
3. The number of independent components is equal to the number of observed mixtures

Eq. 4.5

$$s = Wx,$$

where:

W = to the M (unmixing matrix)

4.1.5 Common Average Reference (CAR)

CAR is a spatial filter that creates a common average with the values of all the electrodes and subtract that value from each channel. CAR works as a filter that reduces the activity that is present in large sections of the electrodes. The CAR method has proved to be comparable with the ear-reference method for referencing (McFarland, McCane, David, & Wolpaw, 1997). The CAR was computed with the following equation:

$$V_i^{\text{CAR}} = V_i^{\text{ER}} - \frac{\sum_{j=1}^n V_j^{\text{ER}}}{n} \quad \text{Eq. 4.6}$$

where:

V_i^{ER} = to the potential between the i th channel and the reference

n = to the number of channels in the montage.

After these steps the pre-processed signal was saved in separated files for each participant.

4.1.6 Data segmentation and averaging

Once the signal was preprocessed, first we identify the start and the end of the 3 seconds of RVS stimulation in the photodiode signal. Then we saved the information regarding the start and the end of the events detected in the light signal and added that info to the EEG signal. Then, these epochs on the EEG signal were segmented.

4.1.7 Identify events in photodiode signal

With the use of a photodiode we recorded the light stimulation during the entire session simultaneously and at the same sampling rate as the EEG signal. In the light signal we identify the stimuli by finding large changes in the average signal that correspond to the presentation of the stimuli.

With a custom made script we set a threshold, line red in Figure 4.2, and searched for peaks that crossed that threshold. Once we found a peak that crossed the threshold we evaluated if the 767 following consecutive points also crossed the threshold (768 in total which correspond to the length of the 3 seconds of stimulation). If any of the 767 following points did not cross the threshold we searched for the next point that crossed it and repeated the procedure. If 768 consecutive points crossed the threshold, we consider them to be an event, and we marked the first (green vertical line) and the last (red vertical line) point, that match to the start and the end of the stimuli. We saved that data to later overlap with the EEG signal and use it as a reference for EEG processing.

Most of the 300 trials during the experiment were detected automatically with the above mentioned script that searched for differences in the average light. However, some events were not detected because the change in the signal was small compared with the average light (continuous light). These events were usually events in the low frequencies and low MD conditions of the experiment. This happened in around 10 percent of the total events per participant. For those not detected events, we proceeded to manual detection that consisted on visual inspection for variation in the signal and manual noting the start and the end of each event and then merging those with the automatically detected events. This manual correction was very time consuming and required a considerable amount effort, but we were able to detect successfully the 300 events in all the participants.

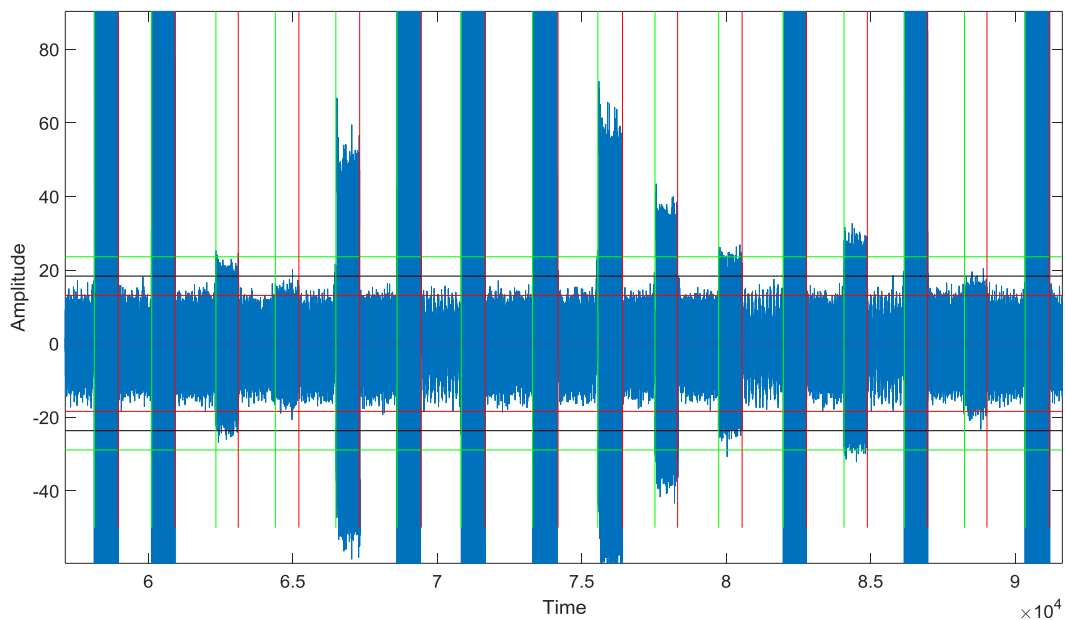


Figure 4.2. Detection of the stimulation events in the photodiode signal. Vertical green and red bars indicated the start and the end of the flickering light stimulation. Horizontal red bars above and below zero indicates the threshold set to identify the events automatically. Horizontal black and green bars were used to identify the events manually after the automatic detection of the

4.1.8 Epochs segmentation

The events detected in the previous step were used to extract epochs from the EEG signal corresponding to the RVS. The EEG signal was separated into non-overlapping epochs of 6 seconds. This period correspond to 3 seconds after the start of stimulation and 3 seconds before the start of stimulation (see Figure 4.3).

4.1.9 Reject epochs

The artifacts were rejected after analyzing the energy of the signal. EEG signal with peaks higher than the sum of the mean of the signal and four times the standard deviation of the signal were rejected in order to exclude trials contaminated with motor or other artifacts. This criteria is represented in the equation 4.7.

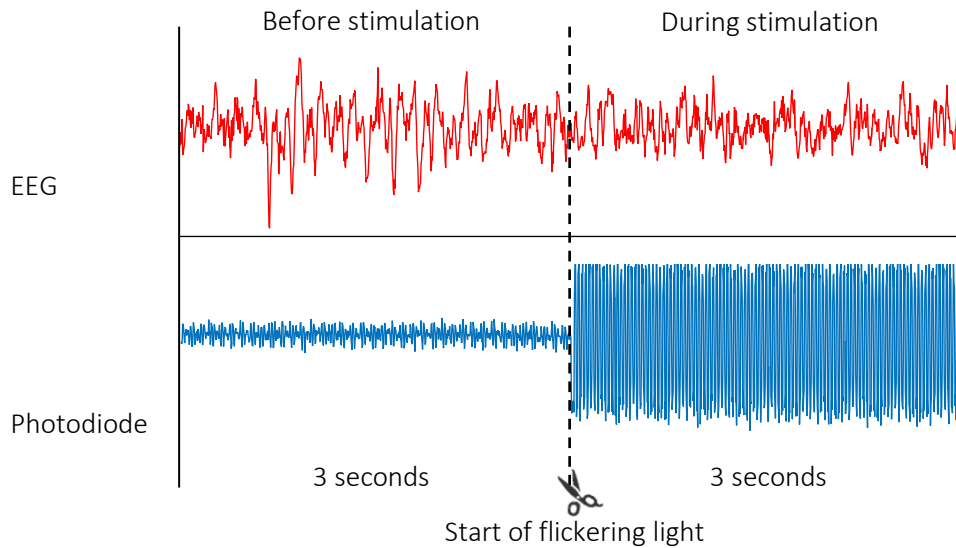


Figure 4.3. Method to segments the epochs. The method consists of detecting the start of the flickering light (stimulation) in the photodiode signal and using it as a reference. Two sets of epochs are created with the reference of 3 seconds, before and after the stimulation.

$$EpochVar < \{meanVar(channel) + 4*stdVar(channel)\}$$

Eq. 4.7

where:

channel = channel number

EpochVar = variance of the current epoch

meanVar(channel) = variance of the mean of the current channel
across all conditions

stdVar(channel) = variance of the standard deviation of the current
channel across all conditions

5 Data Analysis

In the data analysis we followed the procedures employed in the two previous related studies (Van de Sant, et al., 2011; Lazo, et al., 2013) that has been developed in Philips Research because they proved to be effective to detect SSVEP and because this facilitates the combination of their results with ours. The data analysis consisted of the following steps: 1) Power spectral density, 2) Z-score, 3) Equal Error Rates, and 4) Z-score at the Equal Error Rate. This analysis allowed us to estimate the strength of the SSVEP and investigate their relationship with visual perception. This section gives a brief explanation of each method.

5.1 Power Spectral Density (PSD)

PSD is a measure of the power of a signal in the frequency domain. PSD is calculated from the Fast Fourier Transform (FFT) of a signal and it provides a way to characterize the amplitude versus frequency content of the EEG signal.

We applied the FFT into segmented successive time block windows instead of the full epochs. Our epochs had a duration of 3 seconds (768 samples at a sampling rate of 256 Hz): 3 seconds before the start stimulation onset (baseline) and 3 seconds after the start of stimulation (RVS). We used a window of length of 256 samples and an overlap of 128 samples (0.5 seconds). This procedure resulted in 5 half overlapping windows with a length of 256 samples for each 3-second long interval (before and during stimulation).

To plot the data, we selected a channel of interest and take the PSD MATLAB structure, where the values are stored in a 129 length vector. Each data point correspond to one frequency from 1 to 1-128 Hz. Next, we took the mean of the all the PSD epochs that correspond to a condition and we plotted the conditions in the frequency domain. The same procedure was applied for the segments before and after the start of the stimulation. The power of PSD in the plots is represented in $\mu\text{V}^2/\text{Hz}$. The Hz unit depends on the frequency resolution, and in our case it was 0.333 Hz the resolution, so our unit for PSD is $\mu\text{V}^2/0.33 \text{ Hz}$.

5.2 Z-scores

Z-scores (standardized scores) were used to estimate the intensity of the SSVEP response. An individual Z-score was calculated for each trial during stimulation by comparing the PSD log distribution during stimulation with the log PSD baseline. For all the frequencies and MD, each

of their trials was subtracted by the mean of all baseline trials and then divided by the standard deviation of all the baseline trials (see equation below):

$$Zscore = \frac{x - \mu}{\sigma} \quad \text{Eq. 5.1}$$

where:

x = log PSD's epochs of one trial during stimulation

μ = mean of log PSD's epochs of all trials before stimulation

σ = standard deviations of log PSD's epochs of all trials before stimulation

5.3 Equal Error Rate (EER)

To determine whether or not SSVEP were elicited due to the RVS, we found the point at which the probability of type I error is equal to the probability of type II error. This point is the one at which the False Positive (FP) and False Negative (FN) rates are the same. We call this point the Equal Error Rate (EER) and it is calculated according to the equation 5.2 shown below. EER are very useful for biometric systems, like the EEG, to have an optimal identification of the information collected by the device. The lower the equal error rate value, the higher the accuracy of the measurement.

$$EER = p\left(\frac{\mu_1 - \mu_2}{2 * \delta}\right); \quad \text{Eq. 5.2}$$

where:

μ_1 = mean of log PSD's epochs of all trial during stimulation

μ_2 = mean of log PSD's epochs of all trials before stimulation

σ = standard deviations of log PSD's epochs of all trials

5.4 Z-score at the Equal Error Rate (ZEER)

The Z-scores allow to determine the existence of statistically significant difference between two samples that are normally distributed (in our case the log PSD). The multiplication of the standard score and EER gives us a balanced combination of both extracted features to define the measure of the SSVEP intensity.

The measure of the intensity of SSVEP, based on a low standard score can be boosted by the EER in case that the distribution of the samples during and before stimulus has a small overlap. On the contrary, a high SSVEP intensity measure based on a high standard score can be reduced if there is a big overlap in the distributions. The ZEER unit (z-scores at the EER) was computed as follows:

$$\begin{aligned}
 & \text{if } EER \geq 0.5 \text{ or } Z\text{-score} \leq 0 \quad \text{then } ZEER = 0 && \text{Eq. 5.3} \\
 & \text{if } EER \leq 0.5 \text{ or } Z\text{-score} \geq 0 \quad \text{then } ZEER = Z\text{-score} * (1 - EER)
 \end{aligned}$$

5.5 Estimation methods for sensitivity curves

We created sensitivity curves with the use of the behavioral data and the SSVEP signal. The sensitivity curves we created are our approximations to the VPC (Perz, et al., 2011). The sensitivity curves contains the lowest MD necessary for people to perceive the flicker for the behavioral data and to elicit SSVEP for the SSVEP signal. To create these curves we made use of the absolute modulation depth and the psychometric method. We provide a description of these methods in the following paragraphs.

5.5.1 Absolute Modulation Depth (AMD) method

The AMD method finds the lowest MD for a certain frequency that passes a predefined threshold. We set this threshold at 50% of the total responses for a condition (a frequency and a MD) for both behavioral responses and SSVEP. This 50% detection rate in “yes/no” task is often called detection threshold and it is considered not to be reached by guessing (Rose, Teller, & Rendleman, 1970). Moreover, this threshold has used in previous related studies (Lazo, et al., 2013; Perz, et al., 2011; Van de Sant, et al., 2011).

In the case of behavioral responses, for a condition, the threshold was reached when in at least half of the trials participants indicated that they perceived flicker (i.e. 5 out of 10 trials). In the case of the SSVEP the threshold was reached when in half of the trials the ZEER values where higher than 0. A ZEER values higher than 0 is an indication than the SSVEP was detected by our method.

5.5.2 Psychometric method (PM)

The Psychometric method makes use of the non-linear square regression model. With the use of regression analysis the observed data is modeled by a parametric function in order to estimate the coefficients of the nonlinear regression function. As in the case of the AMD we set the selection threshold at 50 % of the trials for a condition “yes” responses for behavioral data and 50 % of ZEER values greater than 0 for SSVEP data. The equation for the Psychometric function is shown below:

$$L(x; \alpha, \beta) = \frac{1}{1 + e^{\frac{\alpha-x}{\beta}}} \quad \text{Eq. 5.4}$$

where:

definition range: $x \in (-\infty, +\infty)$
parameter set: $\theta = (\alpha, \beta)$

with:

$\alpha \in (-\infty, +\infty)$ position parameter
 $\beta > 0$ spread parameter

6 Results

In this section we present the results of the analysis of the behavioral and EEG data. The section is divided in three parts corresponding to three different analysis sections. First, we analyzed the electrical brain activity and characterized the SSVEP. Then, we analyzed the behavioral responses, and created sensitivity curves. After that, we created sensitivity curves for the SSVEP data. Finally, we combined our results with the two previously related studies conducted at Philips. The results are organized in the following three sections: 1) SSVEP analysis, 2) Behavioral responses analysis and 3) SSVEP and visual perception.

6.1 SSVEP analysis

The SSVEP analysis included four steps: 1) PSD estimation, 2) Z-score calculation, 3) EER estimation, and 4) ZEER calculation. The analysis allowed us to characterize the SSVEP and have a measure of their strength.

We analyzed our data with three arrangement of electrodes: 1) Average of P3, Pz, P4, O1, Oz and O2; 2) Individual Pz, and 3) Individual Oz. We selected and presented the results of only Pz as it shows most consistent results and strong SSVEP response in the middle compared to the other arrangements: SSVEP were stronger in Oz and weaker on the average arrangement of electrodes. However, we also included the results corresponding to the analysis of Oz in the Appendix A.

6.2 PSD

We compared the PSD during stimulation against the PSD before stimulation, which is regarded as the baseline. Peaks during stimulation compared with the baseline indicate higher PSD power as a result of the stimulation (Figure 6.1).

Peaks were observed at 37, 48 and 60 Hz for the MD 0.6x and 0.8x the VPT. The three lowest frequencies (7, 13, and 19 Hz) did not have noticeable peaks for any of the MDs. In addition, it can be seen that for frequencies below 20 Hz there is a decrease in power during stimulation compared with the baseline.

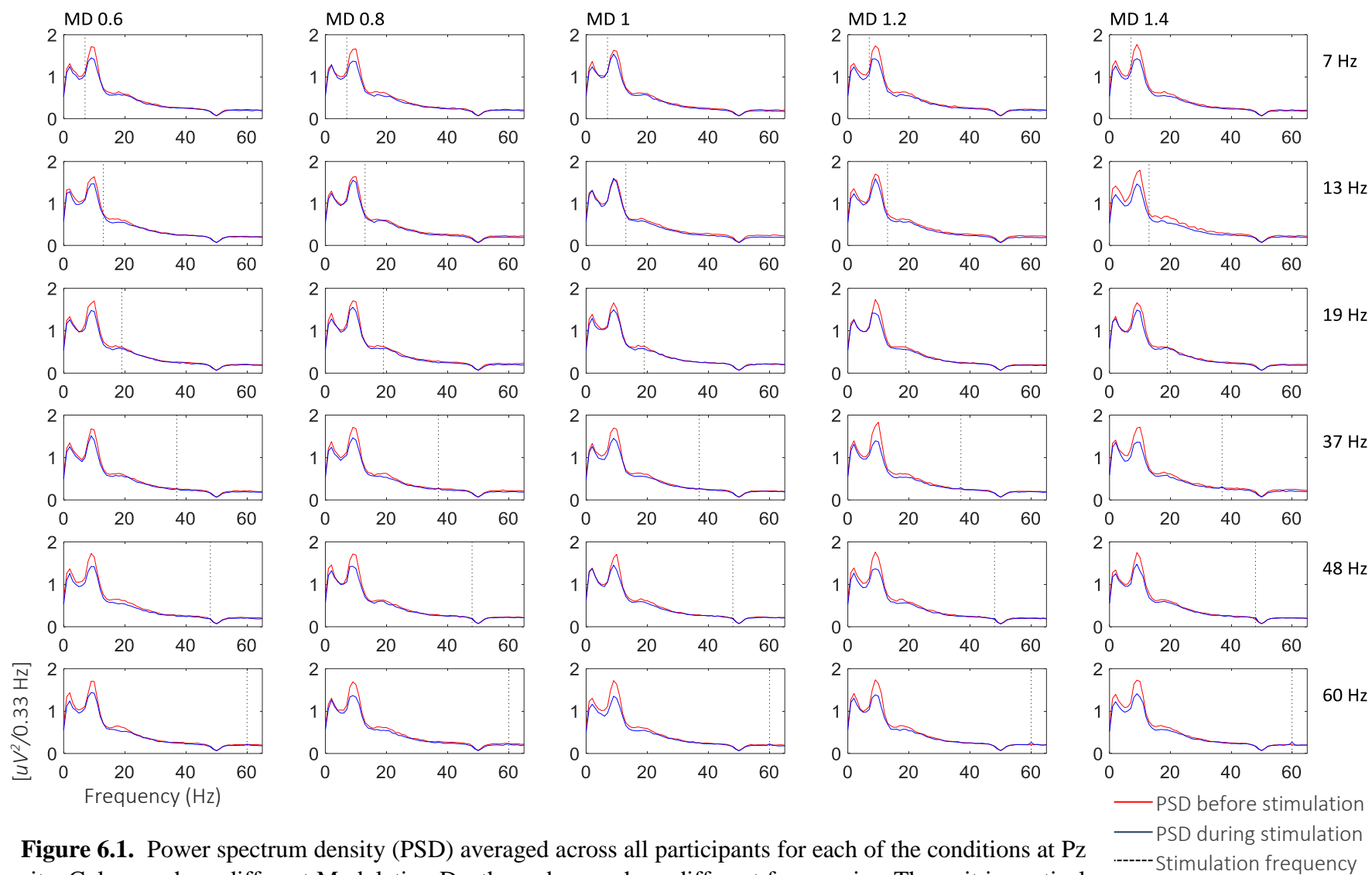


Figure 6.1. Power spectrum density (PSD) averaged across all participants for each of the conditions at Pz site. Columns show different Modulation Depths and rows show different frequencies. The unit in vertical axis is $[\mu V^2/0.33 \text{ Hz}]$ and in the horizontal axis is $[\text{Hz}]$. Red and blue line represent the PSD before and during stimulation respectively. Black dotted line represents the frequency of stimulation.

In order to provide a more precise visualization the PSD, a single condition is depicted in the Figure 6.2. The Figure correspond to the Pz site at 60 Hz and at the MD 1.4x VPT. It can be seen that during stimulation there is a peak at 60 Hz, which is the frequency of stimulation. In addition, there is a decreased at frequencies below 20 Hz as the result of stimulation.

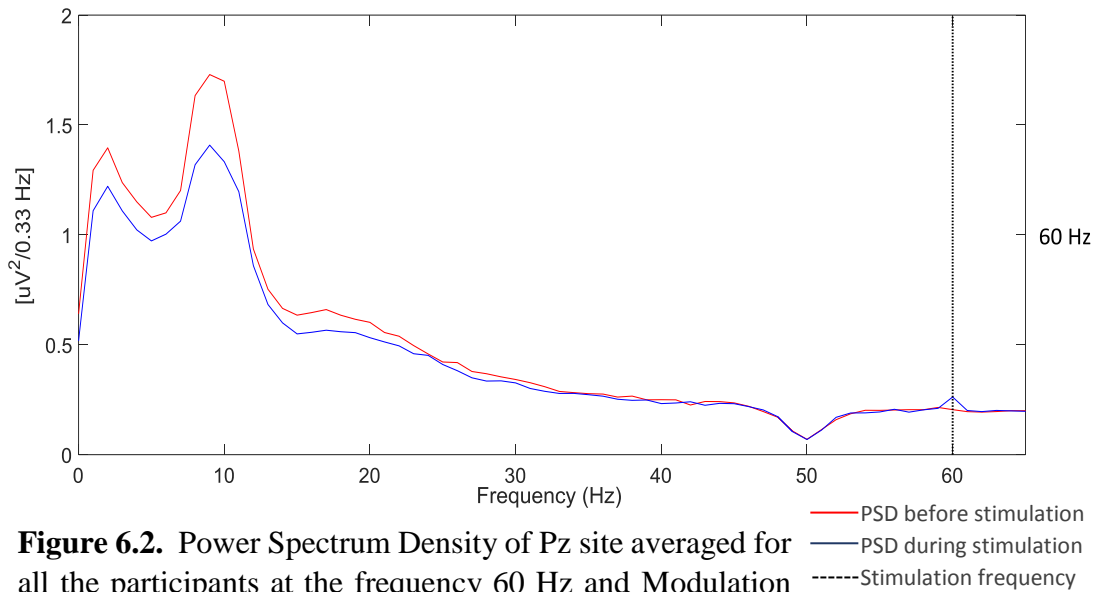


Figure 6.2. Power Spectrum Density of Pz site averaged for all the participants at the frequency 60 Hz and Modulation Depth 1.4 times the Visual Perception Threshold.

6.3 Z-scores

Z-scores were calculated from the PSD during and before stimulation to estimate the strength of the SSVEP. Z-scores peaks above 0 indicate deviations in PSD during stimulation from the PSD baseline as the result of the perception of flickering light (Figure 6.3). For example, at 48 Hz and MD 1.2x VPT, a positive peak is observed at 48 Hz, which correspond to the frequency of stimulation.

Z-scores were larger for higher frequencies and for the higher MDs. Peaks above 0 are observed for frequencies 37, 48 and 60 Hz for MD that are even below 1.0x VPT. For instance, at 48 Hz a peak above 0 is present for MD 0.6x VPT. However, the lowest frequencies 7, 13, 19 Hz, despite that they have peaks at the frequency of the stimulation, they do not have peaks above 0. This can be seen at 13 Hz and for the MD 1.4x VPT.

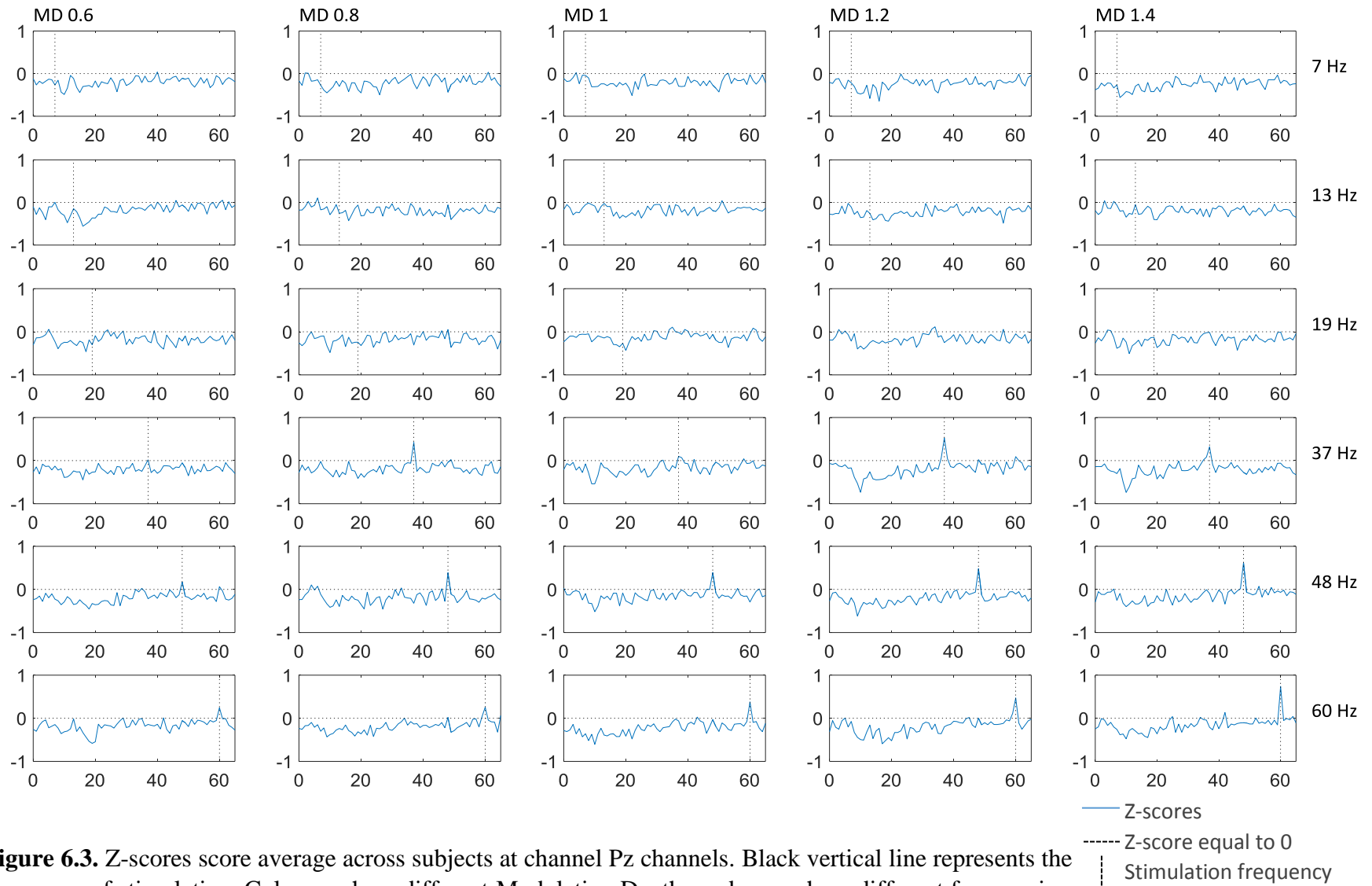


Figure 6.3. Z-scores score average across subjects at channel Pz channels. Black vertical line represents the frequency of stimulation. Columns show different Modulation Depths and rows show different frequencies. The unit in vertical axis is [Z-scores] and in the horizontal axis is [Hz]. Horizontal dotted line was set at the Z-score equal to 0 to help to identify the peaks above 0. Vertical dotted line is at the frequency of stimulation.

To have a visual representation of the spatial distribution of the Z-scores we created a topographic map of these values (Figure 6.4). The plot shows the Z-scores for all channels averaged over all participants and trials for each frequency and MD. The intensity of the colors represent the value of the Z-scores. While colors closer to red represent Z-scores values greater than 0, which represent no change in Z-scores associated to stimulation, colors closer to blue represent Z-scores values less than or equal to 0, which represents no change in Z-scores associated to stimulation.

Sites around the occipital and parietal areas have the higher Z-score values, particularly for the frequencies 37, 48, and 60 Hz and for their highest MDs. The Z-scores in these frequencies show an increase with an increase in MD. Frequencies 7, 13 and 19 Hz do not show Z-score greater than zero across all the frequencies and MD.

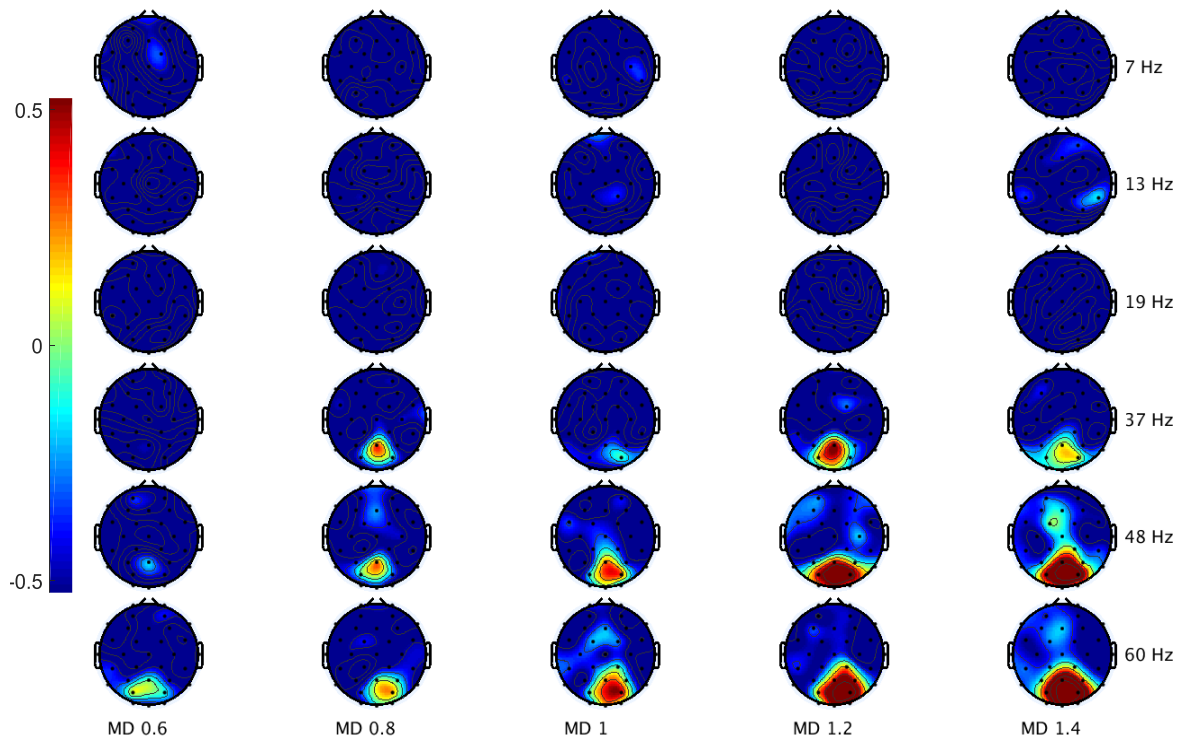


Figure 6.4. Z-scores topo-plots average for all the participants for the 32 channels. Columns show different MD and rows show different frequencies. The color bar is located at the left bounded from 0 (blue) to 0.5 (red).

6.4 EER

To determine whether the effect of the stimulation is significant, we set a criteria base on the EER. EER were obtained analyzing the distributions of the power at the frequency of the

stimulation during stimulation and baseline. As mentioned in the data analysis section the lower the EER the higher the accuracy of the SSVEP detection.

The EERs are displayed in the boxplots in the Figures 6.5, the median is depicted with a red bar and the outliers with blue circles, the box represent the interquartile range between the 25th and 75th percentile. Overall, the three low frequencies 7, 13 and 19 Hz have higher EER than the three high frequencies, as confirmed by their higher medians. There are few outliers across all the conditions. The dispersion of the data is higher in the three highest frequencies compared with the three lowest frequencies. An increase in MD was not associated with either an increase or decrease in the EER values for all the frequencies. For instance, at 60 Hz the EER median is smaller for the highest MD compared with its lowest, but at 19 Hz there are no differences between them.

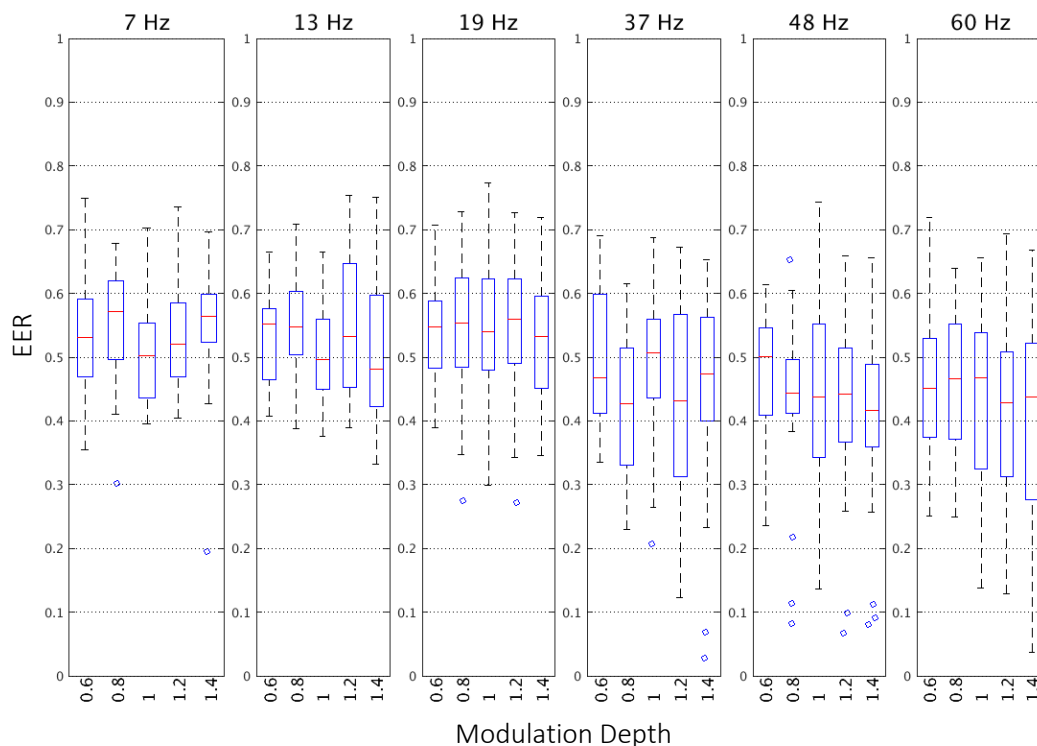


Figure 6.5. Distribution of EER values for Pz site for all the participants by frequency. Boxplots incrementally ordered from left to right. In each boxplot, the distribution and median value for each MD represented by blue color boxes and horizontal red lines respectively. On each box, the edges of the box are the 25th and 75th percentiles. Outliers are plotted individually by small blue circles.

6.5 ZEER

The Z-scores and EER values were combined to create ZEER, a unit that gives a measurement of the strength of the SSVEP on a scale where higher values indicate higher intensity of the

SSVEP. We consider any condition with ZEER values greater than zero to be an indication of SSVEP detection.

The ZEER values for channel Pz are presented in the boxplots in the Figure 6.6. A median above zero is indicative of SSVEP were present. These medians were found for frequencies 37, 48 and 60 Hz for MDs from 0.6x to 1.4x VPT. Medians above zero were also found for the frequency 13 Hz for the MD 1.0 and 1.4 x VPT. The frequencies 7 and 19 Hz did not have a median above zero for any of the MDs.

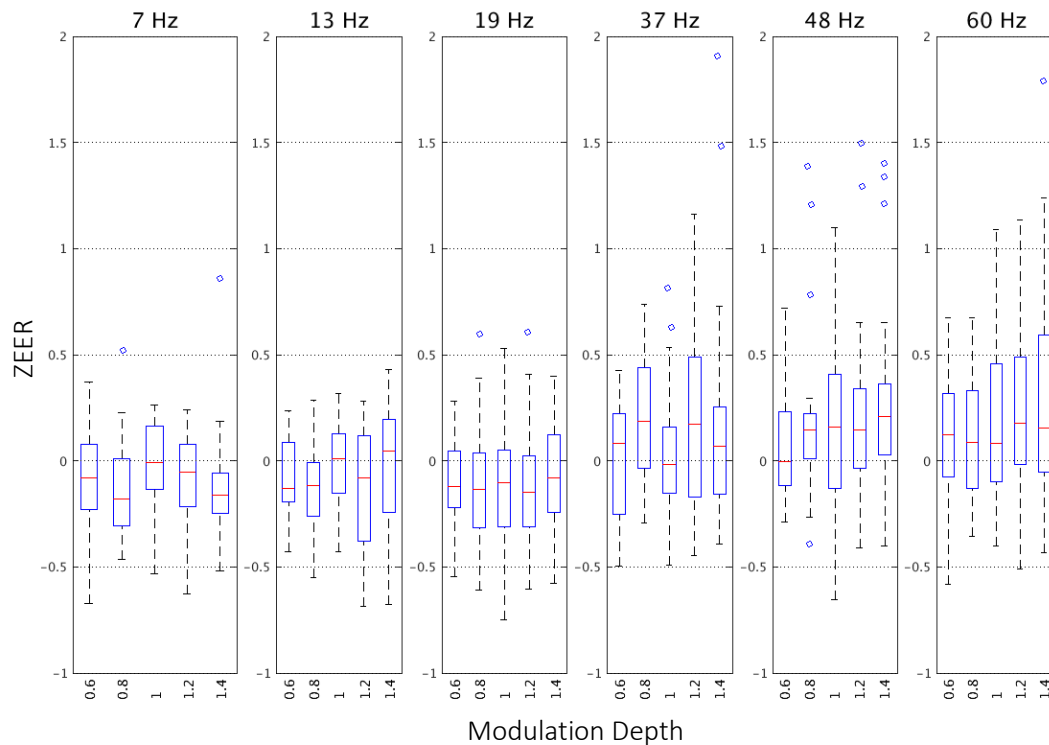


Figure 6.6. Distribution of ZEER values for Pz site for all the participants by frequency. Boxplots incrementally ordered from left to right. In each boxplot, the distribution and median value for each MD represented by blue color boxes and horizontal red lines respectively. On each box, the edges of the box are the 25th and 75th percentiles. Outliers are plotted individually by small blue circles.

The spatial distribution of the ZEER values are plotted in Figure 6.7. The higher ZEER values indicate that SSVEP were detected and are visualized in color closer to red. While ZEER values closer to zero, indicative that SSVEP has not been detected, are visualized in colors closer to blue. Higher ZEER values were found for the three highest frequencies at their highest MDs and for sites around the occipital and parietal sites. Among those conditions, the highest ZEER values were found for the frequency 60 Hz at its MDs 1.2x and 1.4x the VPT. The three lowest frequencies showed almost no variations in ZEER values with the increase of MD for any of the sites.

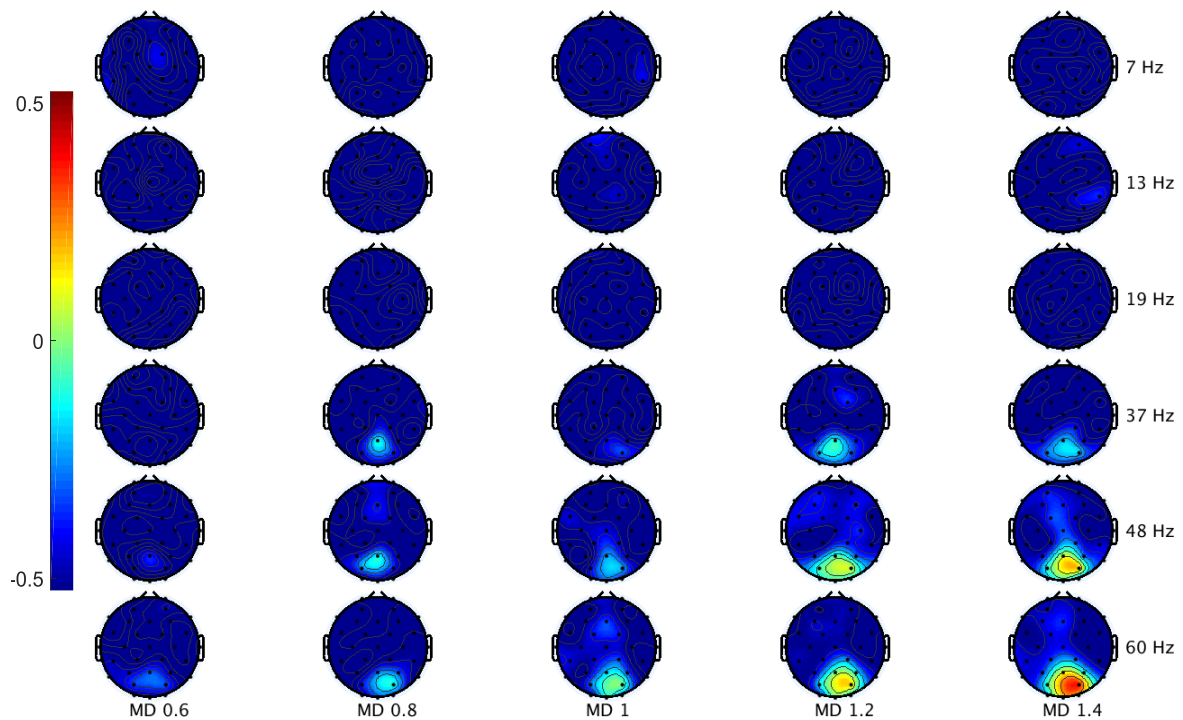


Figure 6.7. ZEER topoplots average for all the participants for the 32 channels. Columns show different MD and rows show different frequencies. The color bar is located at the left bounded from 0 (blue) to 0.5 (red).

6.6 Sensitivity curves estimation for behavioral responses

The sensitivity curves estimated for the behavioral responses with the AMD and Psychometric method are shown in the following sections.

6.6.1 AMD method for behavioral responses

The perception rates obtained with the AMD method are shown in Table 6.1. The Table have colored in blue the lowest MD at which participants reached a perception rate of 0.5. The perception rate is the number of “yes” responses that participants gave to the question do they perceive flicker in the RVS and it goes from 0 to 1.0. A “yes” response is an indication that participants perceived the flicker in the stimulation. It was expected that participants reach the 0.5 perception rate at the MD 1.0x VPT, which was the MD at which they reached that rate in the VPC (Perz, et al., 2011).

The perception rate of 0.5 was reached below the VPT for four out of the six frequencies. At MD 0.8x VPT for 7 Hz and 60 Hz and at MD 0.6x VPT for 37 Hz and 48 Hz. The threshold was not reached for the frequencies 13 and 19 Hz, not even for MD above the VPT. For all the frequencies an increase in MD was associated with an increase in the perception rate, even for those frequencies that did not reach the 0.5 perception rate.

Table 6.1

Average number of “yes” for all participants per condition.

MD	Frequency (Hz)					
	7	13	19	37	48	60
0.6	1.9	0.7	0.6	5.1	5.3	2.5
0.8	5.2	0.7	0.9	7.7	8.2	5.3
1	7.3	1.1	0.8	8.9	9.0	7.0
1.2	7.8	1.9	1.9	9.4	9.1	8.5
1.4	8.9	3.9	3.2	9.8	9.5	9.0

Note. Blue is the lowest modulation depth at which participants reached 5 trials with “yes” responses.

The lowest MD for each frequency that reached a perception rate of at least 0.5 were used to create an AMD sensitivity curve. The AMD curve is plotted together with the VPC (Perz, et al., 2011) for comparison in Figure 6.9. The AMD curve for behavioral responses has a relatively good approximation to the VPC for four out of the six frequencies. The AMD curve resembles the VPC as the MD necessary to have perceivable stimuli increase with frequency and that increase is larger for frequencies above 40 Hz. However, the AMD curve is incomplete for frequencies 13 and 19 Hz because the 0.5 perception rate was not reached.

6.6.2 Psychometric method for behavioral responses

The curves created with the Psychometric method for each frequency are depicted in Figure 6.8. The 0.5 perception rate was estimated to be below the VPT for four frequencies. At MD below 0.6 x VPT for 37 Hz and 48 Hz, below MD 0.8x VPT for 7 Hz, and at MD 0.8x MD for 60 Hz. For frequencies 13 and 19 Hz the 0.5 perception rate was estimated to be above the highest MD 1.4x VPT.

The estimated MDs at which the 0.5 perception rates were estimated were used to create a Psychometric sensitivity curve. The Psychometric curve is plotted with the VPC in Figure 6.11. The shape of the Psychometric curve was very similar to the VPC because it shows an increase in MD with the increase in frequency, and this increase is higher for frequencies above 40 Hz. For frequencies higher than approximately 33 Hz the curve estimated with the Psychometric method has VPT lower than the VPC.

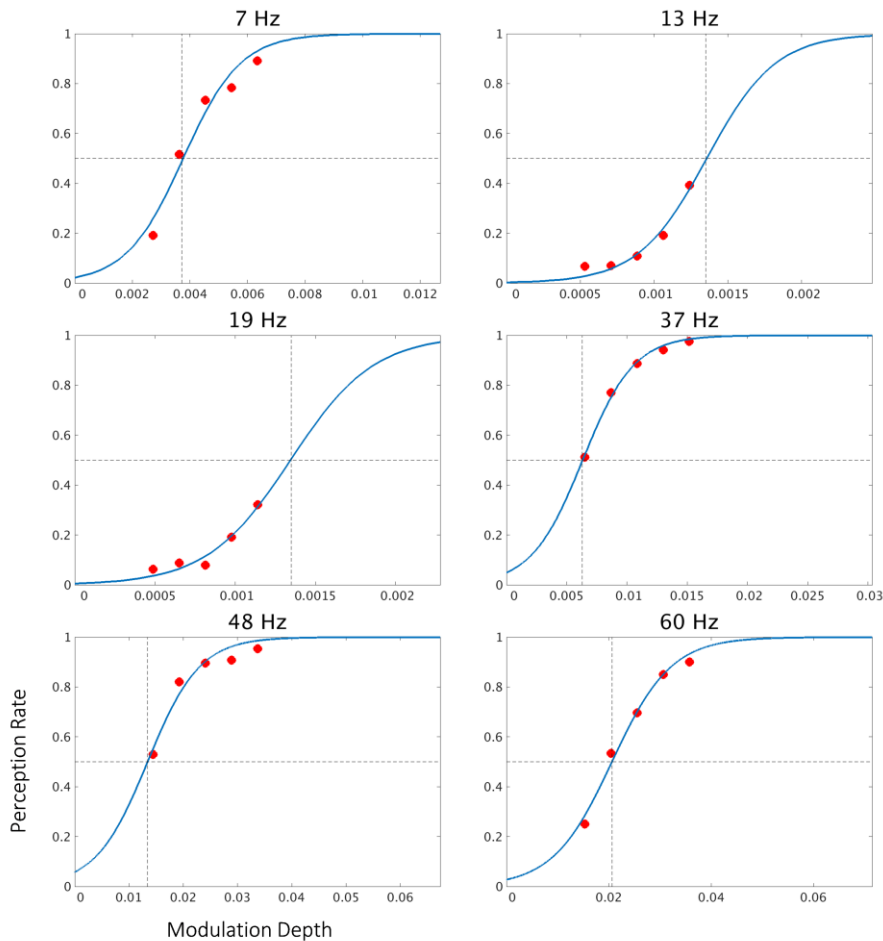


Figure 6.8. Psychometric curves for each frequency and their corresponding Modulation Depths (MD). Red dots represent the perception rate for each MD. Horizontal black dotted line is plotted at the 0.5 perception rate, and black dotted line is at the MD at associated with the perception rate of 0.5.

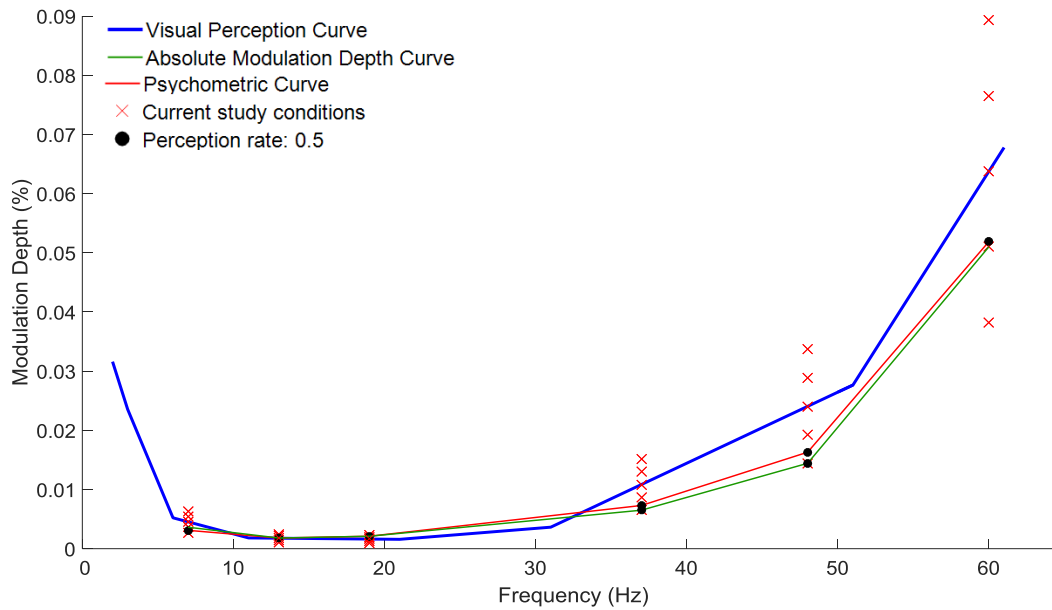


Figure 6.9. Visual Perception Curve and the Absolute Modulation and Psychometric Method curves for behavioral responses. Black dots indicate the smallest modulation depth (MD) at which participants reach a perception rate of 0.5 Red cross marks represent the MD for each of frequency.

6.7 Sensitivity curves estimation for SSVEP

The ZEER values were used to quantify the rate of SSVEP detection for a given condition. We assumed that SSVEP were found for a condition if at least 50% of the trials (5 out of the 10 trials) have ZEER values greater than zero.

6.7.1 AMD method for SSVEP

SSVEP were detected for the three highest frequencies for MDs below the VPT. At MD $0.8x$ VPT for 37 Hz and 48 Hz and at MD $0.6x$ VPT for 60 Hz. For the three lowest frequencies the 0.5 perception threshold was not reached for any MD. The AMD data for SSVEP are shown in Table 6.2.

Table 6.2*Average number of trials with ZEER values greater than 0 for Pz site*

MD	Frequency (Hz)					
	7	13	19	37	48	60
0.6	3.7	3.5	3.6	4.2	4.8	5.0
0.8	3.3	3.3	3.8	5.7	5.2	5.4
1	4.5	4.1	3.7	4.8	5.1	5.4
1.2	3.7	3.2	3.1	5.6	5.5	5.6
1.4	3.6	4.0	3.7	5.3	5.3	5.8

Note. Blue is the lowest modulation depth at which participants reached 5 trials with ZEER values greater than 0.

6.7.2 Psychometric method for SSVEP

The Psychometric method was applied to the ZEER values and individual curves were created for each frequency, they are displayed Figure 6.10. The curves for frequencies 19, 37, 48 and 60 Hz show a positive slope: an increase in ZEER with an increase in MD. The lowest MD necessary to elicit SSVEP for 48 and 60 Hz is estimated to be above the MD 1.0x VPT, but within the range of MD used in this study. For the frequencies 19 and 37 Hz the MD is expected to be above MD 1.4x VPT. For frequencies 7 and 13 Hz the SSVEP data did not allow to estimate the MD at which the 0.5 perception threshold could be reached.

The MDs estimated with the Psychometric method for SSVEP were used to create a SSVEP Psychometric Curve. The SSVEP Psychometric Curve is plotted with the VPC in the Figure 6.11. At high frequencies this curve has lower MD than the VPC, but for low frequencies the MDs are higher, particularly at 7 Hz. The estimated curve is incomplete as the 0.5 perception rate was not possible to estimate for frequencies 13 and 19 Hz.

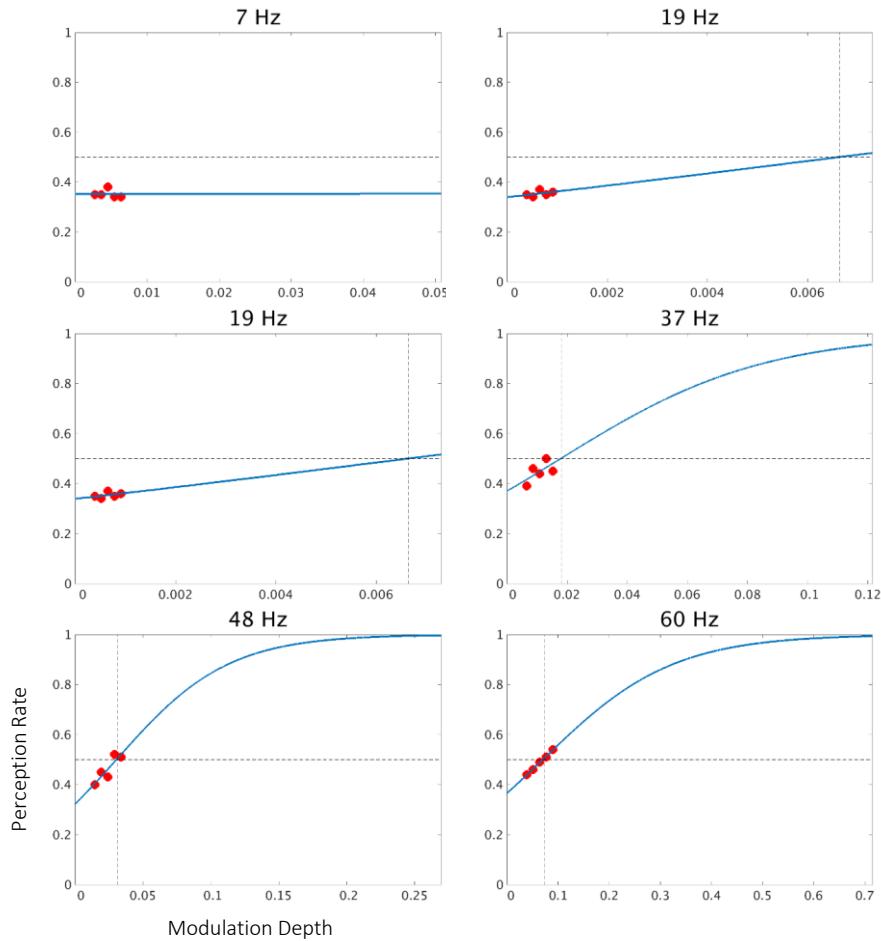


Figure 6.10. ZEER- Psychometric curves for each frequency and their corresponding Modulation Depths (MD). Red dots represent the perception rate for each MD. Horizontal black dotted line is plotted at the 0.5 perception rate, and black dotted line is at the MD at associated with the perception rate of 0.5.

6.7.3 SSVEP and Behavioral curves

The VPC was plotted with the SSVEP Psychometric curve and the AMD and Psychometric curves for behavioral responses (Figure 6.11). Regarding their shape the three curves of this study have a similar shape to the VPC – an increase of MD with the increase of frequency, which is particularly higher for frequencies above 40 Hz. The AMD and Psychometric behavioral curves have MD very close to the VPT. The SSVEP Psychometric curve has MD higher than the VPT at low frequencies. It is remarkable the similarity between the behavioral and SSVEP curves at the frequencies 37 and 48 Hz as the difference between the MDs of both curves is very small.

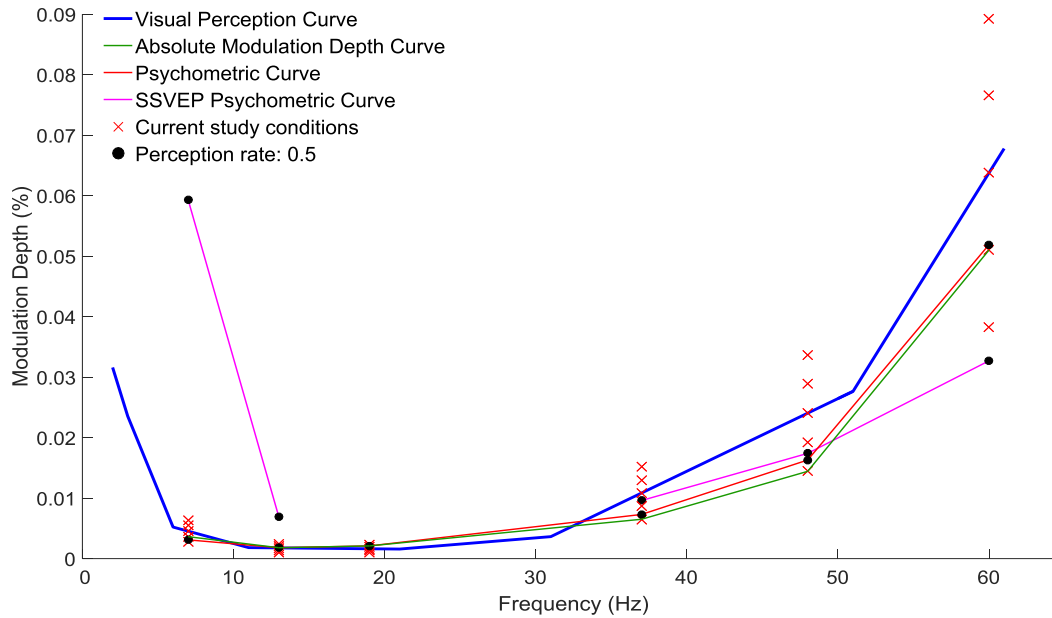


Figure 6.11. Visual Perception Curve, Absolute Modulation Depth Curve, Psychometric Curve, and SSVEP Psychometric Curve for **Pz**. Black dots indicate the smallest modulation depth (MD) at which participants reached a perception rate of 0.5. Red crosses marks represent the MD for each of frequency.

6.8 SSVEP curves in the current and previous studies

We combined the results of the current study with the two previous related studies (Van de Sant, et al., 2011; Lazo, et al., 2013) in order to have more conditions around the VPC and with that have better approach to estimate a SSVEP contrast sensitivity curve. We used ZEER values to determine if SSVEP were presented for a particular condition. We created curves using the AMD and Psychometric method and plotted them separately in two Figures 6.12 and 6.13 respectively. The Figures contain curves estimated and conditions for each study, the VPC, and the VPT at which participants reached the 0.5 perception rate.

6.8.1 SSVEP AMD curves for current and previous studies

The SSVEP-AMD curves for the three studies are depicted in Figure 6.12. The three curves at frequencies higher than 24 Hz have MD close to the VPC (1.0x VPT). For frequencies 37 Hz and above the MDs necessary to elicit SSVEP were found to be below the VPC, with the exception of 40 Hz that was found below and above the VPC (Van de Sant and the current study respectively). For frequencies 24 and 32 Hz MD were found above the VPC. Finally, SSVEP were not found for frequencies below 24 Hz in any MD for any of the three studies.

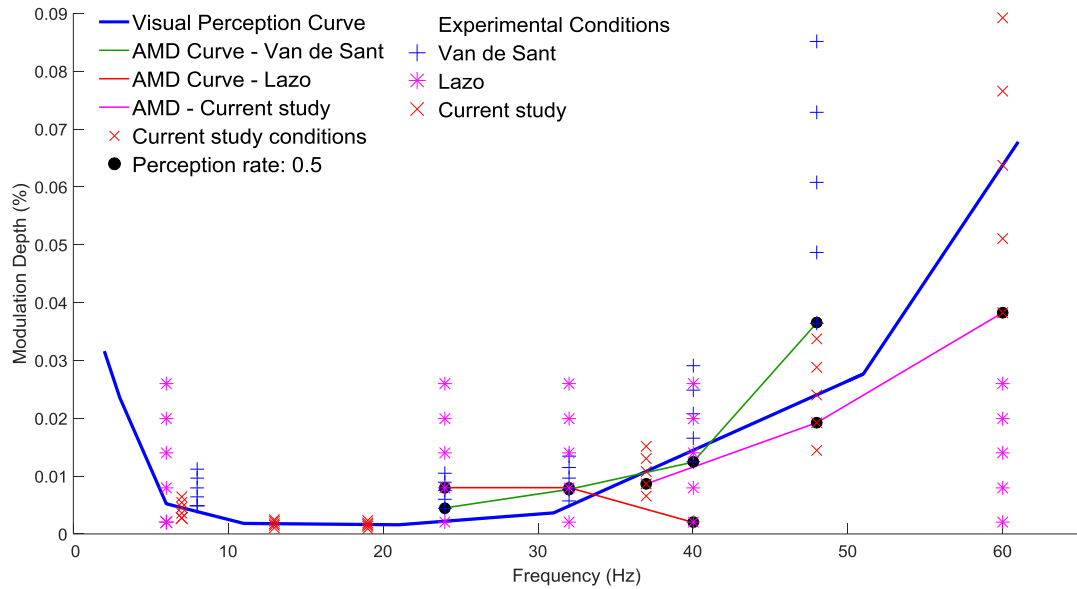


Figure 6.12. Visual Perception Curve, and Absolute Modulation Depth Method Curves of Van de Sant, et al., (2011); Lazo, et al., (2013); and Current study. The experimental conditions are plotted for each study and are represented with blue crosses for Van de Sant, pink stars for Lazo and red cross marks for the current study. Black dots indicate the smallest modulation depth (MD) at which participants reached a perception rate of 0.5.

6.8.2 SSVEP-Psychometric curves for current and previous studies

The Psychometric-SSVEP curves for the three studies are shown in Figure 6.13. As in the case of the AMD the curves are close to the VPC for frequencies above 24 Hz. The curves in the three studies are very close to the VPC for frequencies above 24 Hz. The shape of the curves is very similar to the VPC and even has a similar pattern of a large increase in MD for frequencies above 40 Hz. As with the AMD curves the exception was found at 40 Hz in Lazo's study that has a MD below the VPT. In addition, we predicted using the Psychometric function the MD at which entrainment could be found for 7 and 19 Hz. In both cases the MD is higher than the VPC, but for 7 and 6 Hz is much greater than two times the VPT.

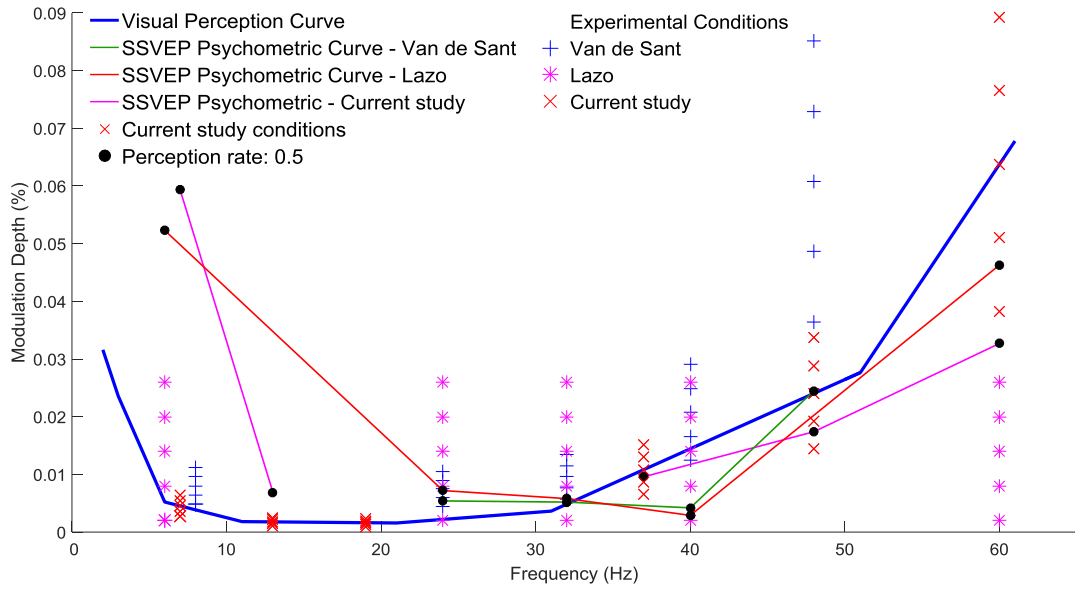


Figure 6.13. Visual Perception Curve, and SSVEP Psychometric Curve of Van de Sant, et al., (2011); Lazo, et al., (2013); and Current study. The experimental conditions are plotted for each study, a blue cross for Van de Sant, pink start for Lazo and red cross marks for the current study. Black dots indicate the smallest modulation depth (MD) at which participants reached a perception rate of 0.5.

7 Discussion

In this work, we focused on studying the relationship between the VPC and SSVEP. Our goal was to investigate whether or not SSVEP could be elicited for frequencies in the range of 7 to 60 Hz by MDs around their corresponding VPT in order to find the lowest MD at which SSVEP can be elicited. We also aimed at identifying how the frequency and MD of the RVS affect the SSVEP response. Our final goal was to create a contrast sensitivity curve for SSVEP similar to the VPC. To this end, we used a flicker detection task with RVS at a wide range of frequencies and MDs around the VPC. We defined a metric (i.e. the ZEER) to quantify the intensity of the SSVEP. In addition, we combined our results with two previous related studies, which allowed us to have a greater number of conditions around the VPC.

SSVEP were elicited for MD around the VPT for our three highest frequencies. The MD for these frequencies (37, 48, and 60 Hz) were below the VPC, namely 0.8x the VPT. Consistent with visual perception research, we found out that the relationship between frequency and MD involves an increase in MD with an increase in frequency: higher MDs were required for SSVEP detection at higher frequencies. For instance, the lowest MD that elicited SSVEP at 60 Hz is more than double the lowest MD that elicited SSVEP at 38 Hz. In addition, the estimated contrast sensitivity curve for SSVEP has a similar shape to the VPC. Both curves show an increase of MD with an increase in frequency and this increase is particularly large for frequencies greater than 40 Hz. The SSVEP contrast sensitivity curve shares characteristics with the VPC: both have similar shape, and the lowest MD eliciting SSVEP or triggering flicker perception are close.

We did not find SSVEP at our three lowest frequencies for any MD. In these frequencies an increase in MD was not associated with an increase in SSVEP ZEER values. Similar results were also observed in the two previous studies. We hypothesize that in order to find SSVEP at low frequencies the required MD is much higher than the VPT. The results from the Psychometric method are in line with this hypothesis as the estimated MD at 7 Hz is larger than double of the VPT. We believe that the reason why an increase in MD did not affect SSVEP was because the difference in MD at low frequencies was very low due to our choice of conditions and the range we covered fell below the one estimated by the Psychometric method. For instance, at 60 Hz the absolute difference between the lowest and highest MD was 0.05156, while at 7 Hz was 0.00363. The sensitivity thresholds for SSVEP at low frequencies seem to be much higher than the VPT.

One explanation why the MD needed to elicit SSVEP at low frequencies appears to be higher comes from the phase reset hypothesis and the synchronization and desynchronization of alpha. The low frequencies in our study and in particular the lowest frequency (7 Hz), which according to the estimations of the Psychometric method require a MD much larger than the VPC are close to the Alpha range. The Alpha band is the most dominant frequency in the EEG of adults and in the occipital lobe (Klimesch, 1999). It may be possible that stimulation at much higher MD is necessary for SSVEP manifestation in order to reset (phase alignment) the ongoing oscillation in that frequency range. Because Alpha is the most dominant band, it may recruit more neurons than the other bands, so stronger stimulation in the alpha range may be necessary compared with higher frequencies so that a larger number of neurons start to oscillate in synchrony with the stimulation.

In the PSD analysis a decrease in power was observed in frequencies lower than 20 Hz, this decrease was larger for higher MD. It seems that this power decrease, desynchronization, in the ongoing EEG activity is a result of stimulation. In addition, alpha desynchronization is related to the difficulty of the task, the more difficult the task the more desynchronization (Başar, Schürmann, Başar-Eroglu, & Karakaş, 1997). However, our results appear to be in the opposite direction because with an increase in MD participants were more likely to detect flicker, which suggests that they find the task easier with higher MD. However, it may be that at low MDs participants did not make an effort to identify the flicker as the light appeared to be continuous. While, at high MDs when the flicker was more visible participants made an effort to identify the flicker.

The spatial distribution of the SSVEP response appeared consistent with other studies in the field (Pastor, Artieda, Arbizu, Valencia, & Masdeu, 2003). We found that most SSVEP activity was localized over occipital and parietal sites and there were only little propagation to frontal areas. This is not surprising considering that SSVEP are artefacts of a visual process (Herrmann, 2001) and do not involve higher cognitive processes in a large extent. Our results indicate that the SSVEP response we have found in our experiment was mainly related to visual processing.

Behavioural responses were also aligned with existing research. We found that the subjective visual perception in our frequencies were very close to the VPC. The MDs at which participants were able to perceive the flicker were around the VPT for all frequencies and the curves based on behavioural data had a very similar shape to the VPC. In addition, an increase

in MD was associated with a higher perception rate. This suggests that our task was appropriate to evaluate perception of RVS.

Our results suggest that SSVEP responses are sensitive to visual perception laws but some differences exist for the low and high frequency range. To strengthen this hypothesis additional research is needed especially in the low frequency range. As mentioned above, the MD thresholds at low frequencies may lie above the VPC. To get further insights on that matter, we propose a follow up study evaluating only frequencies in the low range (6 to 24 Hz) consisting of 2 stages. In the first stage, we propose to explore a wide range of MD by using exponential proportions of the VPC: 1, 2, 4, 8, 16, and 32 times the VPT. Then in the second stage, we propose to use proportions of the MD where SSVEP were found in order to find the MD closest to the VPT. We consider that such study would allow for a more comprehensive sampling of the frequency MD space and complement of the results of the current and the previous studies for the creation of the SSVEP contrast sensitivity curve.

We were able to elicit SSVEP around the VPC but only for high frequencies. We found that the MD necessary to elicit SSVEP are very close to the VPC for high frequencies, and it is even below the VPC. Moreover, the shape of our estimated SSVEP contrast sensitivity curve is very similar to the VPC, they both have an increase of MD with an increase in frequency and that increase is larger for frequencies higher than 40 Hz. Overall, our findings can contribute to the development of contrast sensitivity curve for SSVEP, which despite the increasing use of SSVEP in research and practical applications does not exist. Such sensitivity curve will help to develop a more diverse variety of stimuli, using more frequencies and MDs. This would increase the conditions that could be used to elicit distinct SSVEP. For instance, for a frequency the MD can be varied to create SSVEP with different amplitudes. This can help to designing finer stimuli eliciting SSVEP and helping to evaluate the visual system as well as increase the diversity of RVS for SSVEP-BCI based systems.

8 References

- Adrian, E. D., & Matthews, B. H. C. (1934). The interpretation of potential waves in the cortex. *The Journal of Physiology*, *81*(4), 440-471.
- Başar, E., Schürmann, M., Başar-Eroglu, C., & Karakaş, S. (1997). Alpha oscillations in brain functioning: an integrative theory. *International journal of psychophysiology*, *26*(1), 5-29.
- Bayram, A., Bayraktaroglu, Z., Karahan, E., Erdogan, B., Bilgic, B., Özker, M., ... & Arikan, K. (2011). Simultaneous EEG/fMRI analysis of the resonance phenomena in steady-state visual evoked responses. *Clinical EEG and neuroscience*, *42*(2), 98-106.
- Bergholz, R., Lehmann, T. N., Fritz, G., & Rütger, K. (2008). Fourier transformed steady-state flash evoked potentials for continuous monitoring of visual pathway function. *Documenta Ophthalmologica*, *116*(3), 217-229.
- Bi, L., Fan, X. A., & Liu, Y. (2013). EEG-based brain-controlled mobile robots: a survey. *Human-Machine Systems, IEEE Transactions on*, *43*(2), 161-176.
- BioSemi products. (2016, July 16). Retrieved from <http://www.biosemi.com/products.htm>
- Capilla, A., Pazo-Alvarez, P., Darriba, A., Campo, P., & Gross, J. (2011). Steady-state visual evoked potentials can be explained by temporal superposition of transient event-related responses. *PLoS one*, *6*(1), e14543-e14543.
- Delorme, A., & Makeig, S. (2004). EEGLAB: an open source toolbox for analysis of single-trial EEG dynamics including independent component analysis. *Journal of neuroscience methods*, *134*(1), 9-21.
- Di Russo, F., Pitzalis, S., Aprile, T., Spitoni, G., Patria, F., Stella, A., ... & Hillyard, S. A. (2007). Spatiotemporal analysis of the cortical sources of the steady-state visual evoked potential. *Human brain mapping*, *28*(4), 323-334.
- Di Russo, F., Spinelli, D., & Morrone, M. C. (2001). Automatic gain control contrast mechanisms are modulated by attention in humans: evidence from visual evoked potentials. *Vision research*, *41*(19), 2435-2447.
- Fisher, R. S., Harding, G., Erba, G., Barkley, G. L., & Wilkins, A. (2005). Photic-and Pattern-induced Seizures: A Review for the Epilepsy Foundation of America Working Group. *Epilepsia*, *46*(9), 1426-1441.
- Gray, M., Kemp, A. H., Silberstein, R. B., & Nathan, P. J. (2003). Cortical neurophysiology of anticipatory anxiety: an investigation utilizing steady state probe topography (SSPT). *Neuroimage*, *20*(2), 975-986.
- Herrmann, C. S. (2001). Human EEG responses to 1–100 Hz flicker: resonance phenomena in visual cortex and their potential correlation to cognitive phenomena. *Experimental brain research*, *137*(3-4), 346-353.
- Hyvärinen, A., Karhunen, J., & Oja, E. (2004). What is Independent Component Analysis? In A. Hyvärinen, J. Karhunen, & E. Oja. (Eds.) *Independent component analysis* (pp. 146-164). New York, NY: John Wiley & Sons.
- Ishiguro, Y., Takada, H., Watanabe, K., Okumura, A., Aso, K., & Ishikawa, T. (2004). A Follow-up Survey on Seizures Induced by Animated Cartoon TV Program “Pocket Monster”. *Epilepsia*, *45*(4), 377-383.

- Kelly, D. H. (1961). Visual responses to time-dependent stimuli. I. Amplitude sensitivity measurements. *JOSA*, *51*(4), 422-429.
- Klimesch, W. (1999). EEG alpha and theta oscillations reflect cognitive and memory performance: a review and analysis. *Brain research reviews*, *29*(2), 169-195.
- Krolak-Salmon, P., Hénaff, M. A., Tallon-Baudry, C., Yvert, B., Guénot, M., Vighetto, A., ... & Bertrand, O. (2003). Human lateral geniculate nucleus and visual cortex respond to screen flicker. *Annals of neurology*, *53*(1), 73-80.
- Kuller, R., & Laike, T. (1998). The impact of flicker from fluorescent lighting on well-being, performance and physiological arousal. *Ergonomics*, *41*(4), 433-447.
- Lazo, M., Tsoneva, T., & Garcia Molina, G. (2013). *EEG-based characterization of flicker perception*. Technical Report. Eindhoven, NB: Philips Research Europe.
- Luck, S. J. (2014). An introduction to the event-related potential technique. In S. J. Luck (Eds.), *An Introduction to Event-Related Potentials and Their Neural Origins* (pp. 1-50). Cambridge, MA: MIT press.
- Makeig, S., Westerfield, M., Jung, T. P., Enghoff, S., Townsend, J., Courchesne, E., & Sejnowski, T. J. (2002). Dynamic brain sources of visual evoked responses. *Science*, *295*(5555), 690-694.
- McFarland, D. J., McCane, L. M., David, S. V., & Wolpaw, J. R. (1997). Spatial filter selection for EEG-based communication. *Electroencephalography and clinical Neurophysiology*, *103*(3), 386-394.
- Moratti, S., Clementz, B. A., Gao, Y., Ortiz, T., & Keil, A. (2007). Neural mechanisms of evoked oscillations: stability and interaction with transient events. *Human brain mapping*, *28*(12), 1318-1333.
- Morgan, S. T., Hansen, J. C., & Hillyard, S. A. (1996). Selective attention to stimulus location modulates the steady-state visual evoked potential. *Proceedings of the National Academy of Sciences*, *93*(10), 4770-4774.
- Müller, M. M., Picton, T. W., Valdes-Sosa, P., Riera, J., Teder-Sälejärvi, W. A., & Hillyard, S. A. (1998). Effects of spatial selective attention on the steady-state visual evoked potential in the 20–28 Hz range. *Cognitive Brain Research*, *6*(4), 249-261.
- Nicolas-Alonso, L. F., & Gomez-Gil, J. (2012). Brain computer interfaces, a review. *Sensors*, *12*(2), 1211-1279.
- Norcia, A. M., Appelbaum, L. G., Ales, J. M., Cottreau, B. R., & Rossion, B. (2015). The steady-state visual evoked potential in vision research: A review. *Journal of Vision*, *15*(6), 4-4.
- Pantle, A. (1971). Flicker adaptation—I. Effect on visual sensitivity to temporal fluctuations of light intensity. *Vision research*, *11*(9), 943-952.
- Pastor, M. A., Artieda, J., Arbizu, J., Valencia, M., & Masdeu, J. C. (2003). Human cerebral activation during steady-state visual-evoked responses. *The journal of neuroscience*, *23*(37), 11621-11627.
- Pastor, M. A., Valencia, M., Artieda, J., Alegre, M., & Masdeu, J. C. (2007). Topography of cortical activation differs for fundamental and harmonic frequencies of the steady-state visual-evoked responses. An EEG and PET H215O study. *Cerebral Cortex*, *17*(8), 1899-1905.
- Perlstein, W. M., Cole, M. A., Larson, M., Kelly, K., Seignourel, P., & Keil, A. (2003). Steady-state visual evoked potentials reveal frontally-mediated working memory activity in humans. *Neuroscience letters*, *342*(3), 191-195.

- Perz, M., Sekulovski, D., & Vogels I. (2011). *Flicker perception*. Technical Report. Eindhoven, NB: Philips Research Europe.
- Regan, D. (1966). Some characteristics of average steady-state and transient responses evoked by modulated light. *Electroencephalography and clinical neurophysiology*, 20(3), 238-248.
- Regan, D. (1977). Steady-state evoked potentials. *Journal of the Optical Society of America*, 67(11), 475-1489.
- Regan, D. (1989). Methods for recording Steady-State Evoked Potentials. In D. Regan, (Eds.) *Human Brain Electrophysiology: Evoked Potentials and Evoked Magnetic Fields in Science and Medicine*. (pp. 70-111). New York, NY: Elsevier Science Publishing Co., Inc.
- Rose, R. M., Teller, D. Y., & Rendleman, P. (1970). Statistical properties of staircase estimates. *Perception & Psychophysics*, 8(4), 199-204.
- Sammer, G., Blecker, C., Gebhardt, H., Kirsch, P., Stark, R., & Vaitl, D. (2005). Acquisition of typical EEG waveforms during fMRI: SSVEP, LRP, and frontal theta. *Neuroimage*, 24(4), 1012-1024.
- Sartucci, F., Borghetti, D., Bocci, T., Murri, L., Orsini, P., Porciatti, V., ... & Domenici, L. (2010). Dysfunction of the magnocellular stream in Alzheimer's disease evaluated by pattern electroretinograms and visual evoked potentials. *Brain research bulletin*, 82(3), 169-176.
- Shady, S., MacLeod, D. I., & Fisher, H. S. (2004). Adaptation from invisible flicker. *Proceedings of the National Academy of Sciences of the United States of America*, 101(14), 5170-5173.
- Silberstein, R. B., Schier, M. A., Pipingas, A., Ciorciari, J., Wood, S. R., & Simpson, D. G. (1990). Steady-state visually evoked potential topography associated with a visual vigilance task. *Brain Topography*, 3(2), 337-347.
- Skrandies, W., & Raile, A. (1989). Cortical and retinal refractory periods in the human visual system. *International Journal of Neuroscience*, 44(1-2), 185-195.
- Sokol, S., & Riggs, L. A. (1971). Electrical and psychophysical responses of the human visual system to periodic variation of luminance. *Sciences*, 10(3), 171-180.
- Srinivasan, R., Bibi, F. A., & Nunez, P. L. (2006). Steady-state visual evoked potentials: distributed local sources and wave-like dynamics are sensitive to flicker frequency. *Brain topography*, 18(3), 167-187.
- Srinivasan, R., Fornari, E., Knyazeva, M. G., Meuli, R., & Maeder, P. (2007). fMRI responses in medial frontal cortex that depend on the temporal frequency of visual input. *Experimental brain research*, 180(4), 677-691.
- Teng, F., Chen, Y., Choong, A. M., Gustafson, S., Reichley, C., Lawhead, P., & Waddell, D. (2011). Square or sine: Finding a waveform with high success rate of eliciting SSVEP. *Computational intelligence and neuroscience*, 2011, 2.
- Thorpe, S. G., Nunez, P. L., & Srinivasan, R. (2007). Identification of wave-like spatial structure in the SSVEP: Comparison of simultaneous EEG and MEG. *Statistics in medicine*, 26(21), 3911-3926.
- Trenité, D. K. N., Binnie, C. D., & Meinardi, H. (1987). Photosensitive patients: symptoms and signs during intermittent photic stimulation and their relation to seizures in daily life. *Journal of Neurology, Neurosurgery & Psychiatry*, 50(11), 1546-1549.

Van de Sant, J., Tsoneva, T., Garcia-Molina, G., & Farquhar, J. (2011). SSVEP at single and beating frequencies utilizing perceptual insights. Technical Report. Technical Report. Eindhoven, NB: Philips Research Europe.

Van Erp, J. B., Lotte, F., & Tangermann, M. (2012). Brain-computer interfaces: beyond medical applications. *Computer*, (4), 26-34.

Vanagaite, J., Pareja, J. A., Støren, O., White, L. R., Sand, T., & Stovner, L. J. (1997). Light-induced discomfort and pain in migraine. *Cephalalgia*, 17(7), 733-741.

Vialatte, F. B., Maurice, M., Dauwels, J., & Cichocki, A. (2010). Steady-state visually evoked potentials: focus on essential paradigms and future perspectives. *Progress in neurobiology*, 90(4), 418-438.

Widmann, A., Schröger, E., & Maess, B. (2015). Digital filter design for electrophysiological data—a practical approach. *Journal of neuroscience methods*, 250, 34-46.

9 Appendix A

Figures and tables for Oz channel

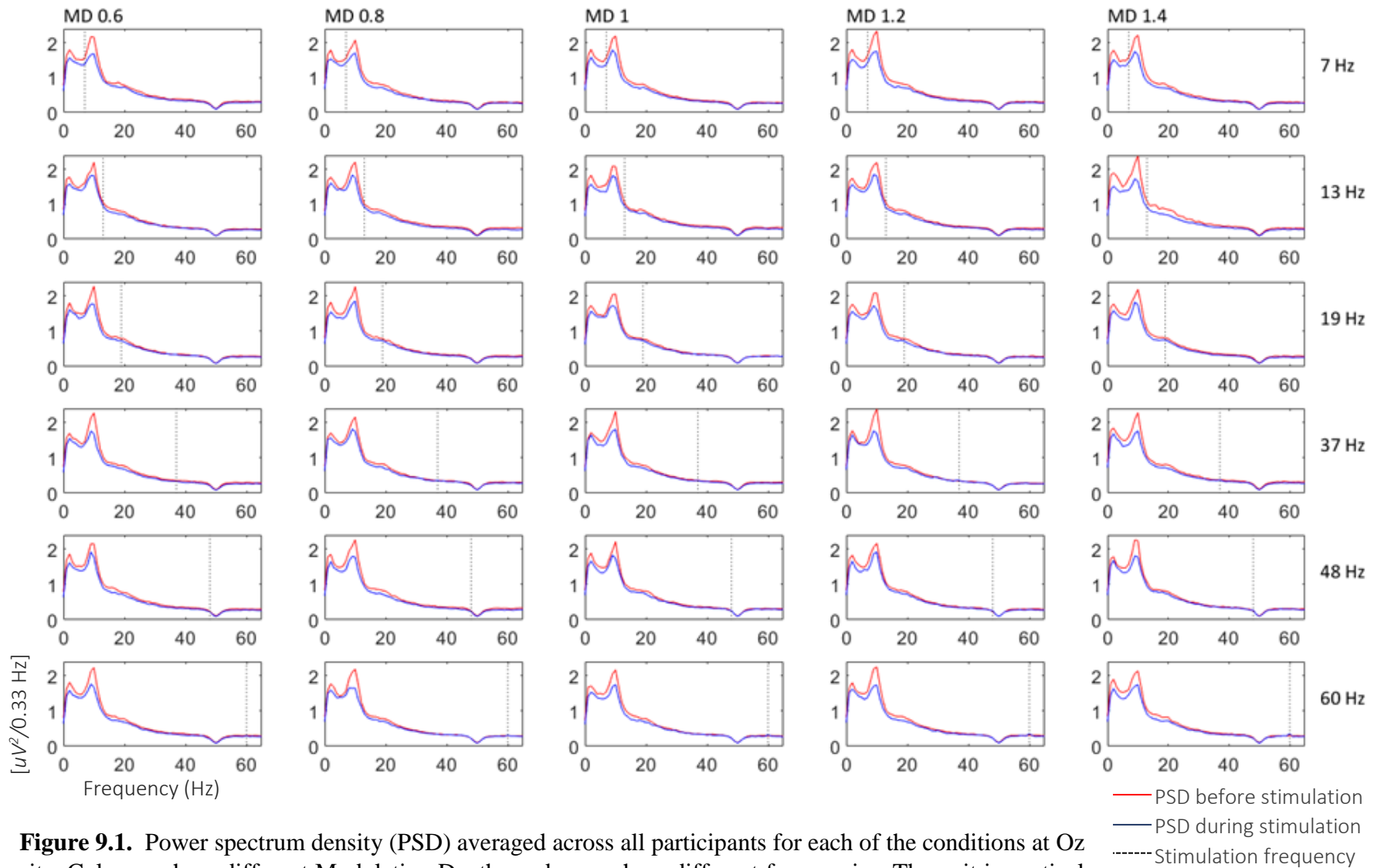


Figure 9.1. Power spectrum density (PSD) averaged across all participants for each of the conditions at Oz site. Columns show different Modulation Depths and rows show different frequencies. The unit in vertical axis is $[uV^2/0.33\text{Hz}]$ and in the horizontal axis is $[\text{Hz}]$. Red and blue line represent the PSD before and during stimulation respectively. Black dotted line represents the frequency of stimulation.

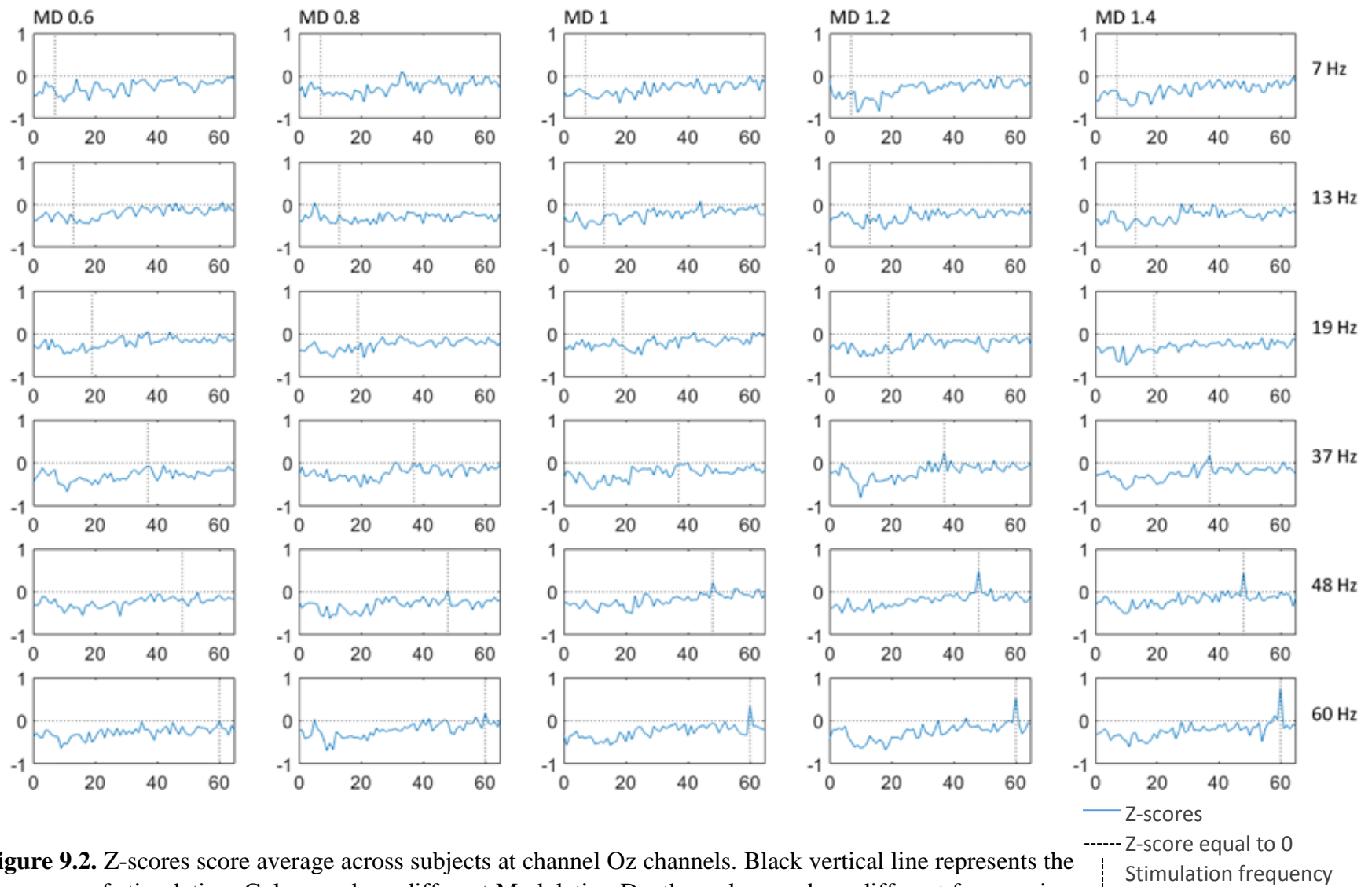


Figure 9.2. Z-scores score average across subjects at channel Oz channels. Black vertical line represents the frequency of stimulation. Columns show different Modulation Depths and rows show different frequencies. The unit in vertical axis is [Z-scores] and in the horizontal axis is [Hz]. Horizontal dotted line was set at the Z-score equal to 0 to help to identify the peaks above 0. Vertical dotted line is at the frequency of stimulation.

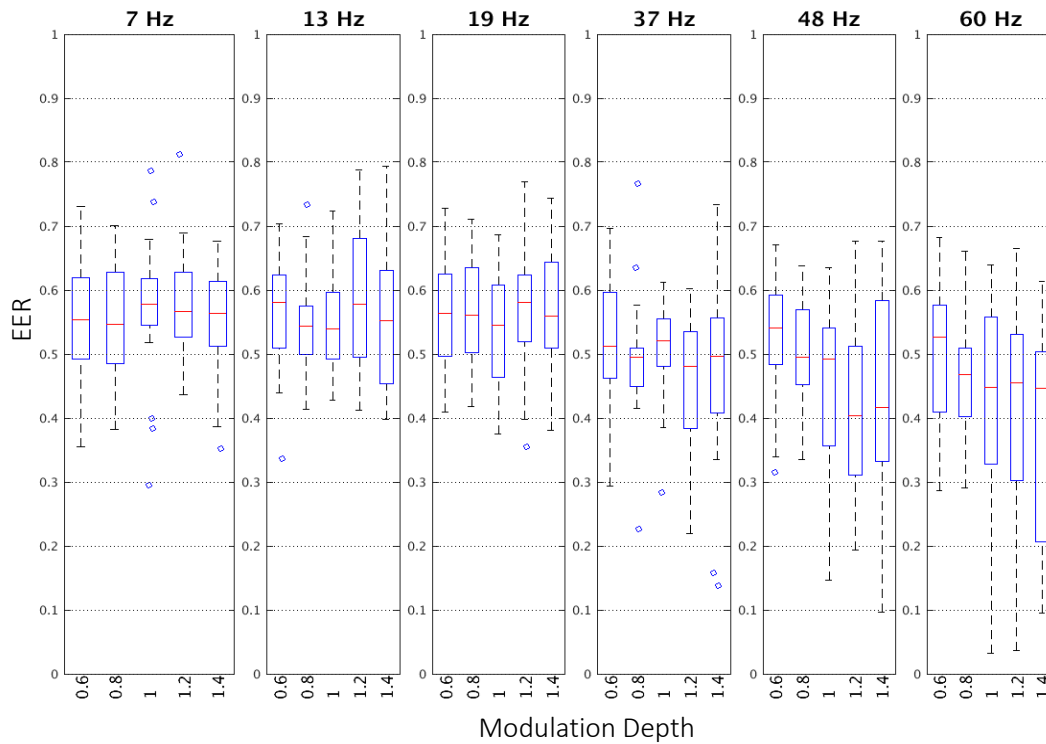


Figure 9.3. Distribution of EER values for Oz site for all the participants by frequency. Boxplots incrementally ordered from left to right. In each boxplot, the distribution and median value for each MD represented by blue color boxes and horizontal red lines respectively. On each box, the edges of the box are the 25th and 75th percentiles. Outliers are plotted individually by small blue circles.

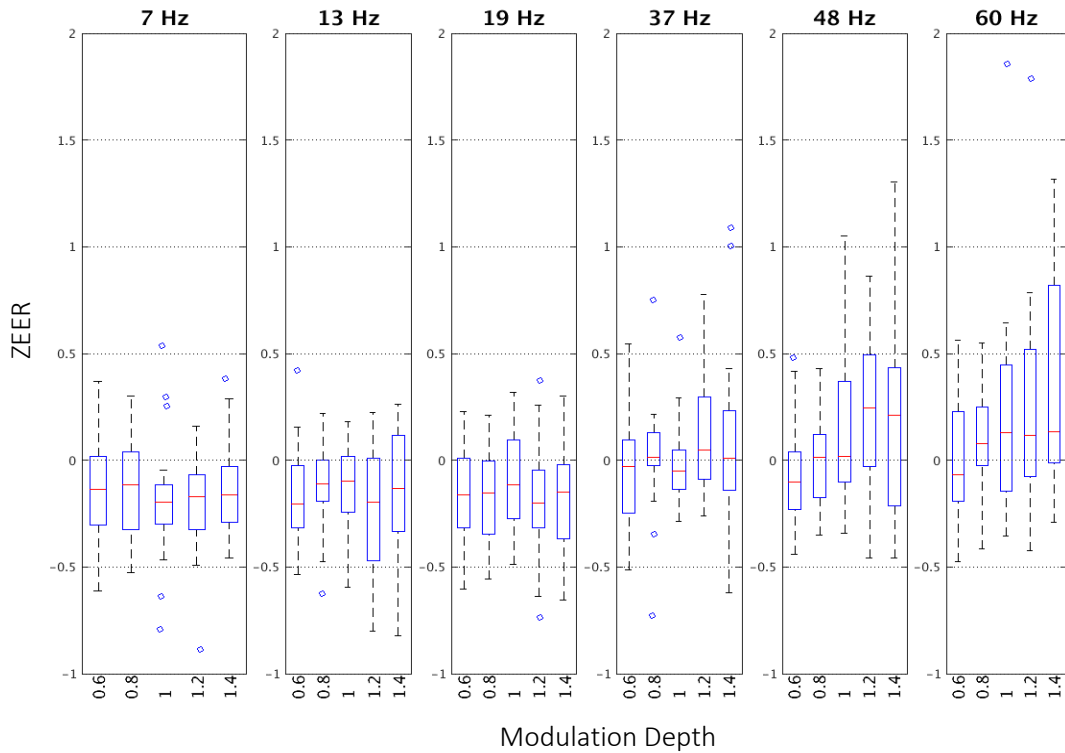


Figure 9.4. Distribution of ZEER values for Oz site for all the participants by frequency. Boxplots incrementally ordered from left to right. In each boxplot, the distribution and median value for each MD represented by blue color boxes and horizontal red lines respectively. On each box, the edges of the box are the 25th and 75th percentiles. Outliers are plotted individually by small blue circles.

Table 9.1*Average number of trials with ZEER values greater than 0 for Oz site*

MD	Frequency (Hz)					
	7	13	19	37	48	60
0.6	3.3	3.3	3.2	4.0	3.8	4.1
0.8	3.6	3.7	3.6	4.9	4.1	4.9
1	3.3	3.0	3.9	4.2	4.5	5.5
1.2	3.0	2.7	3.2	5.0	5.4	5.6
1.4	3.3	3.2	3.5	4.3	5.3	5.9

Note. Blue is the lowest modulation depth at which participants reached 5 trials with ZEER values greater than 0.

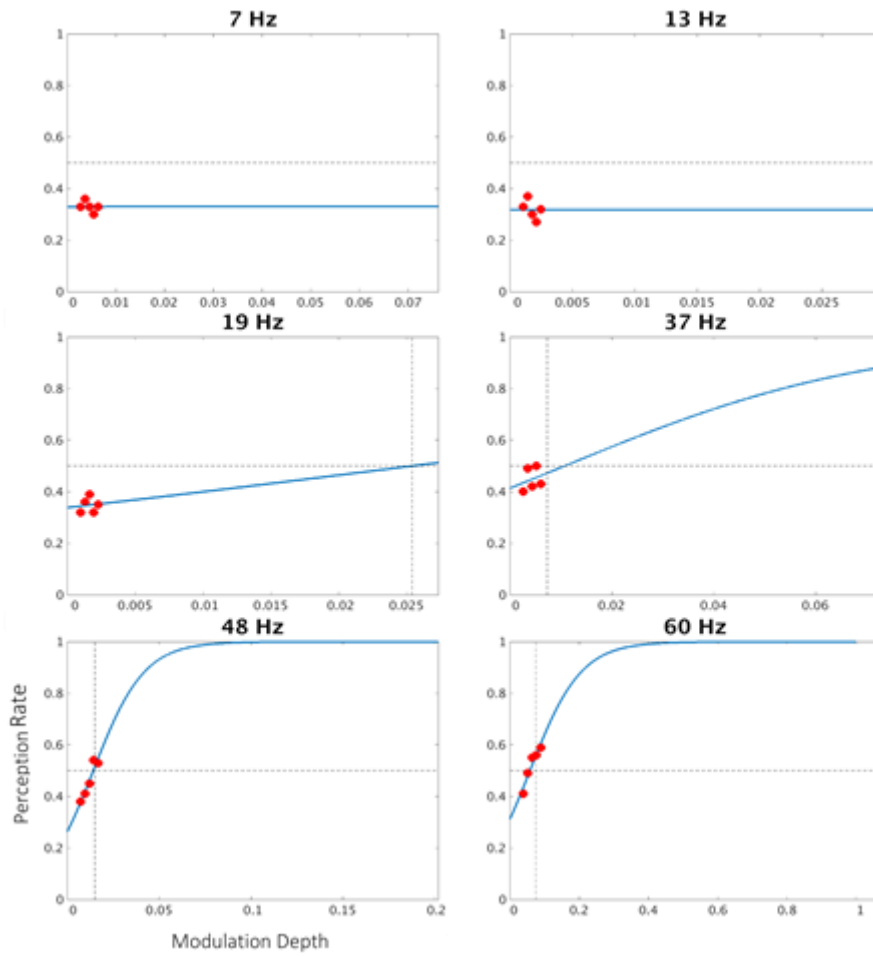


Figure 9.5. Psychometric curves for each frequency and their corresponding Modulation Depths (MD). Red dots represent the perception rate for each MD. Horizontal black dotted line is plotted at the 0.5 perception rate, and black dotted line is at the MD at associated with the perception rate of 0.5.

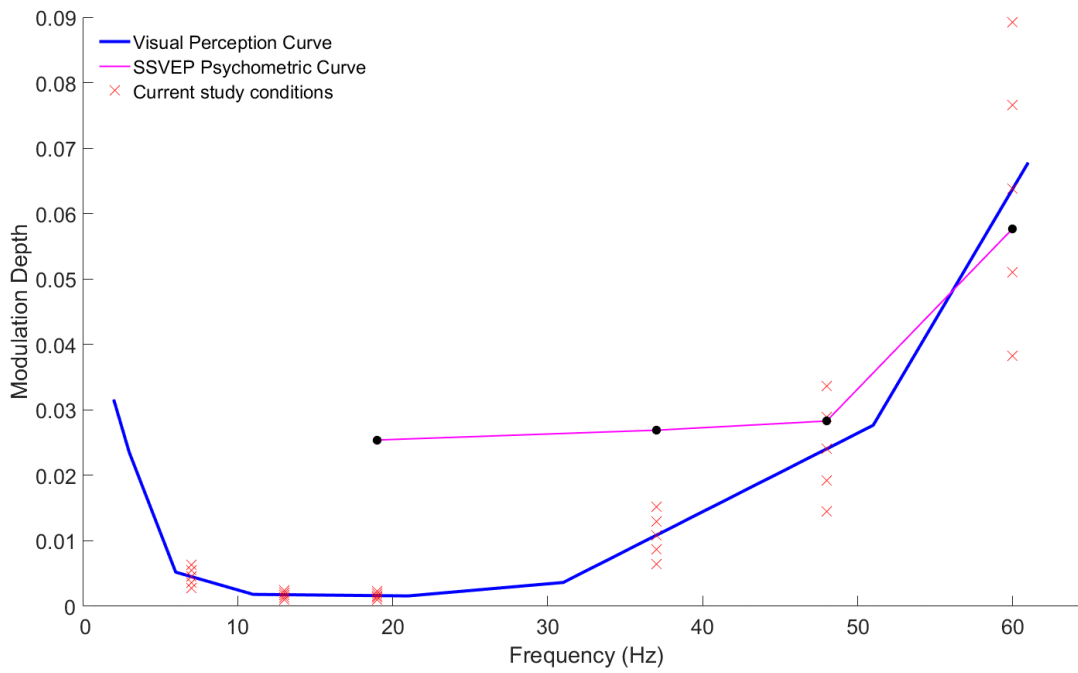


Figure 9.6. SSVEP-Psychometric Curve for Oz and the Visual Perception Curve. Black dots indicate the smallest modulation depth (MD) at which participants reached a perception rate of 0.5. Red crosses marks represent the MD for each of frequency.